Overview of the radiated fraction and radiation asymmetries following shattered pellet injection

IAEA Technical Meeting on Plasma Disruptions and their Mitigation, 20-23 July 2020

(Virtual Meeting)

R. Sweeney[1], L. Baylor[2], D. Bonfiglio[3], D. Craven[4], N. Eidietis[5], R. Granetz[1], V. Huber[6], E. Joffrin[7], E.M. Hollmann[8], S. Jachmich[9], J. Kim[10], D. King[4], M. Lehnen[9], J. Lovell[2], C. Maggi[4], A. Peacock[4], R. Raman[11], C. Reux[7], U. Sheikh[12], D. Shiraki[2], S. Silburn[4], Y. Li[13], J. Wilson[4], DIII-D Team, JET Contributors[a)], and KSTAR Team

[1]Massachusetts Institute of Technology, Cambridge, MA 02139, USA

[2]Oak Ridge National Laboratory, Oak Ridge, TN 37830, USA

[3]Consorzio RFX, Corso Stati Uniti 4, Padova, Italy

[4]UKAEA/CCFE, Culham Science Centre, Abingdon, OX14 3DB, UK

[5]General Atomics, San Diego, CA 92186, USA

[6]Forschungszentrum Jülich GmbH, Supercomputing Centre, 52425 Jülich, Germany

[7]CEA, IRFM, F-13108 Saint Paul Lez Durance, France

[8]University of California-San Diego, La Jolla, CA 92093, USA

[9]ITER Organization, Route de Vinon-sur-Verdon- CS 90 046 -13067 St Paul Lez Durance Cedex - France

[10]National Fusion Research Institute, Daejeon 305-806, South Korea

[11]University of Washington, Seattle, WA 98195, USA

[12]École Polytechnique Fédérale de Lausanne, Swiss Plasma Center, 1015 Lausanne, Switzerland

[13]Huazhong University of Science and Technology, Wuhan 430074, People's Republic of China

[a)]See the author list of E. Joffrin et al., Nucl. Fusion **59** (2019) 112021

E-mail: rsween@mit.edu

Outline

- ITER thermal mitigation requirements
- Axisymmetric radiated fraction calculations
- Limitations of axisymmetric assumption
- Helical radiation structures:
  - DIII-D observations
  - JET observations
- Preliminary 3D radiated energy estimates in JET
- Resolving the toroidal peaking near the injection
- Magnetic control of the radiation asymmetry
- Radiation following dual injection

ITER thermal mitigation requirements

Longevity of the ITER divertor requires high radiated fractions

- Critical heat flux factor for tungsten is $50\ MJ/m^2s^{0.5}$
- Divertor thermal quench (TQ) heat flux area of $23\ m^2$ *, and thermal quench duration of $\tau_{tq} \approx 1$ ms

$$\frac{350\ MJ}{23\ m^2\sqrt{10^{-3}\ s}} = 480\ MJ/m^2s^{0.5}$$

- Conducted heat loads must be less than 10%

Conclusion: more careful analysis** finds thermal radiated fraction $\boldsymbol{f_{rad,th}}$ **must exceed 0.93** ($f_{rad,th} = W_{rad,th}/W_{th}$)

*V. Riccardo et al., Nucl. Fusion **45** (2005)
** M. Lehnen et al., J. Nucl. Mater. **463** (2015)

High radiated fractions reduce divertor loads, but increase first wall loads; longevity of the first wall requires uniform radiation

- The melt temperature of Be is $T_{lim} = 1551$ K, and the first wall can reach $T_{0,fw} = 600$ K
- Maximum allowable peaking factor is*

$$PF \leq \left(T_{lim} - T_{0,fw}\right)\sqrt{\pi\kappa\rho C_p}\sqrt{\tau_{tq}}\,\frac{A_{fw}}{f_{tq}W_{th}}$$

k ≡heat conductivity, ρ ≡mass density, C_p ≡heat capacity per unit mass, A_{fw} ≡first wall area, W_{th} ≡thermal energy

- **$PF \leq 2$ on Be tiles****

*G. Olynyk, MIT Thesis 2013
** M. Lehnen et al., J. Nucl. Mater. **463** (2015)

The goals of SPI thermal mitigation are now defined

ITER requires:

1. $f_{rad,th} \geq 0.93$
2. $PF \leq 2$

Radiated fractions in DIII-D and JET assuming axisymmetry

DIII-D: The thermal radiated fraction $<f_{rad,th}>$ increases with the quantity of injected neon, doubling relative to unmitigated

$< f_{rad,th} > = < W_{rad,th} >/W_{th}$ $< X > \equiv$ X is calculated assuming axisymmetry

- $<f_{rad,th}>$ approaches 0.9
- Strike point temperatures decrease and first wall temperatures increase, consistent with expectation

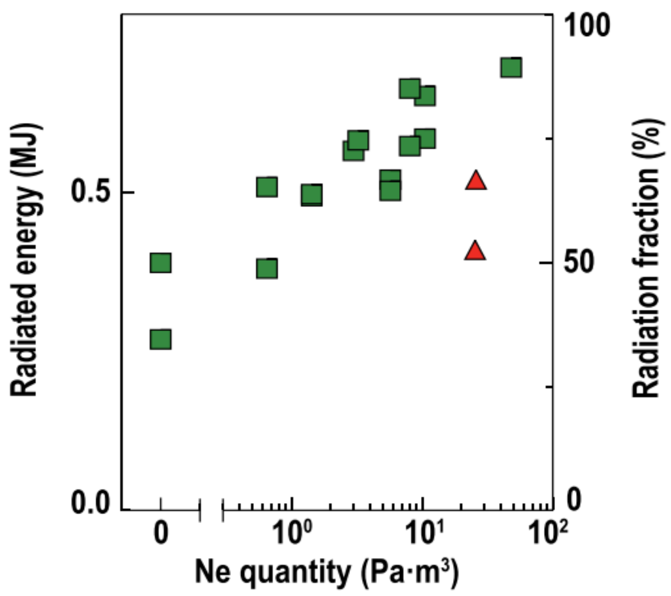

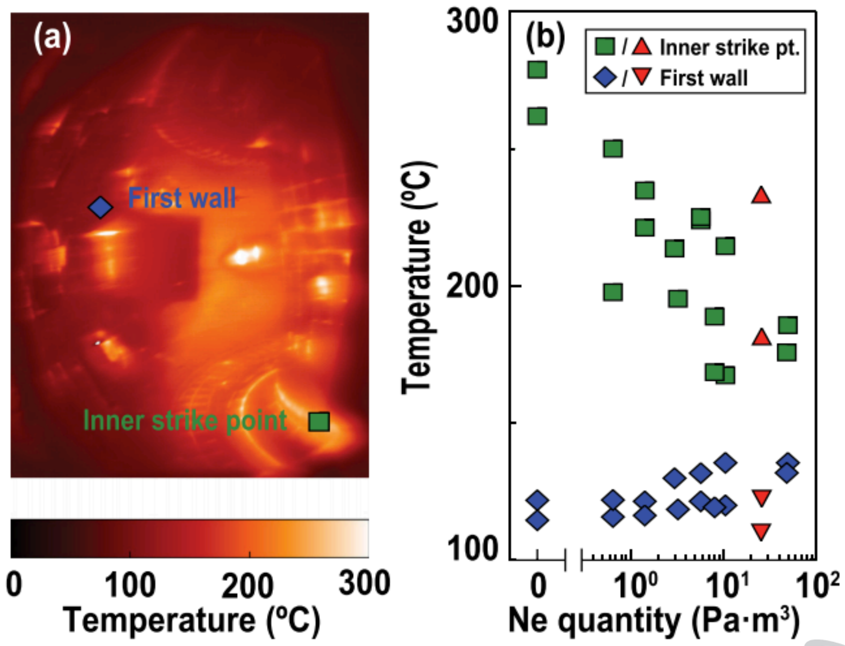

D. Shiraki et al., Phys. Plasmas **23** (2016) 062516

JET: The maximum <f_{rad}> decreases as f_{th} increases with SPI, reproducing previous MGI results

- (Left) Trend originally found with massive gas injection (MGI)
  - Implies <$f_{rad,th}$>~50% at best
- (Right) Trend qualitatively reproduced with SPI

$$< f_{rad,th} > = < W_{rad,th} > / W_{th}$$

$$< f_{rad} > = < W_{rad} > / (W_{th} + W_{mag} - W_{coupled})$$

$< X > \equiv$ X is calculated assuming axisymmetry

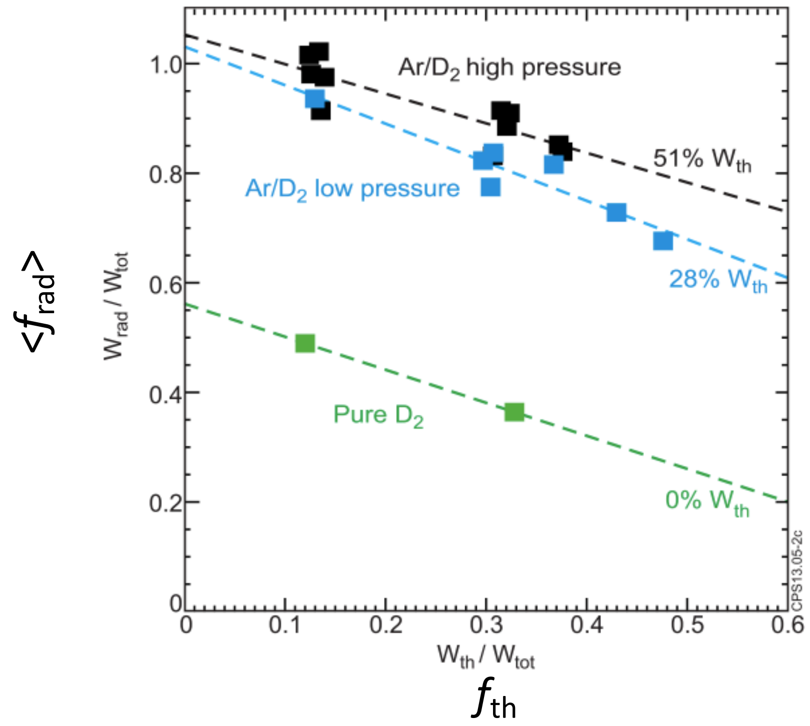

JET SPI Database

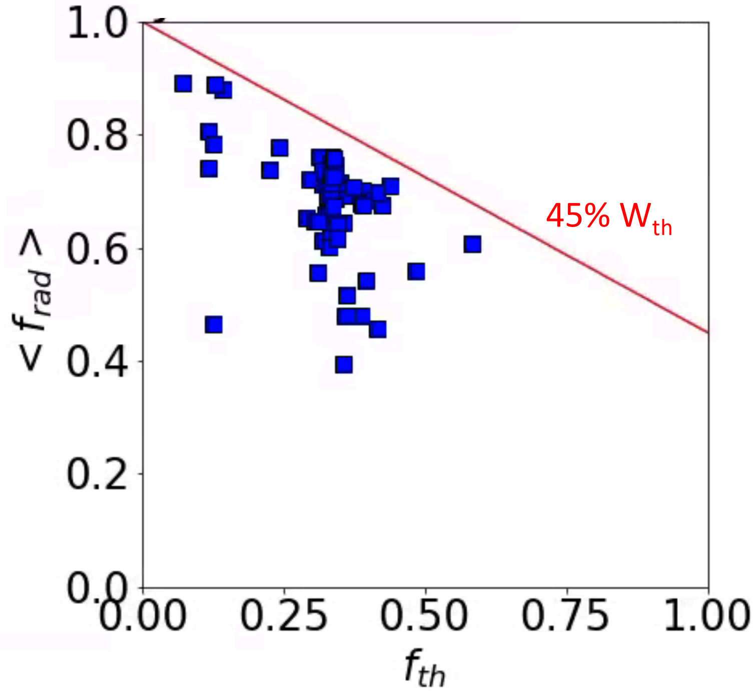

(left) M. Lehnen et al., Nucl. Fusion **53** (2013) 093007

How accurate are the axisymmetric calculations, and is the decreasing <f_{rad}> with f_{th} real?

- The remainder of the talk investigates 3D properties to address these questions

*G. Olynyk, MIT Thesis 2013
** M. Lehnen et al., J. Nucl. Mater. **463** (2015)

Limitations of the axisymmetric assumption (JET case study)

Large errors in P_{rad} can result from uncertainty in the location of the radiation in the poloidal plane

- Errors reach **many tens of percent**, but ITER must achieve **within 10%** of complete radiation!

KB5H

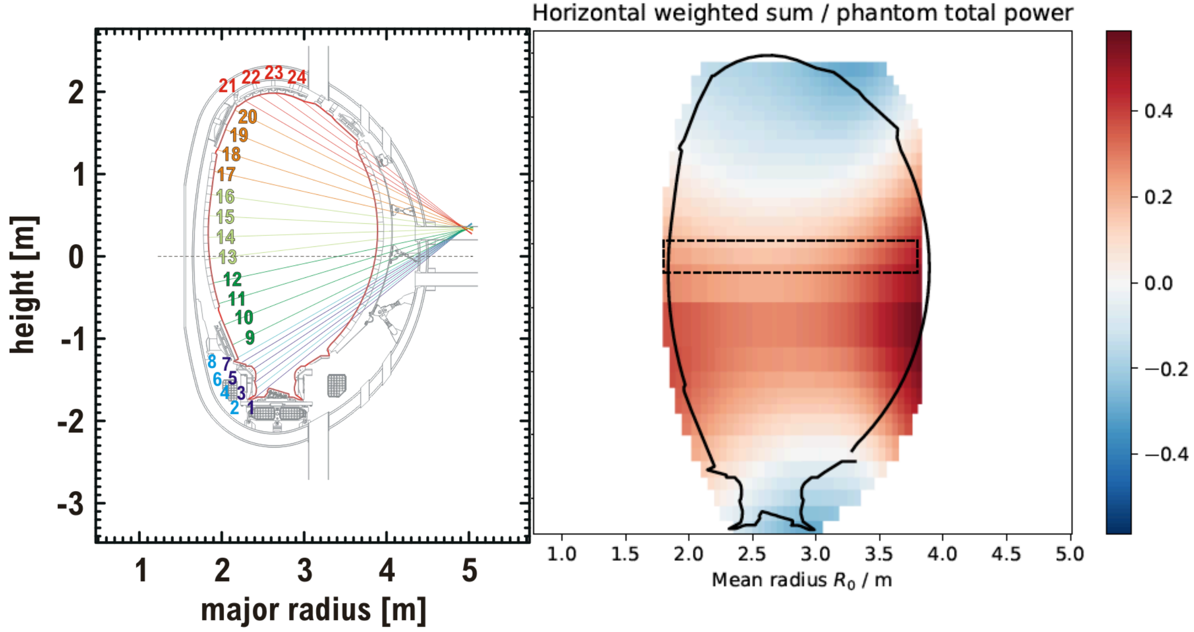

KB5V

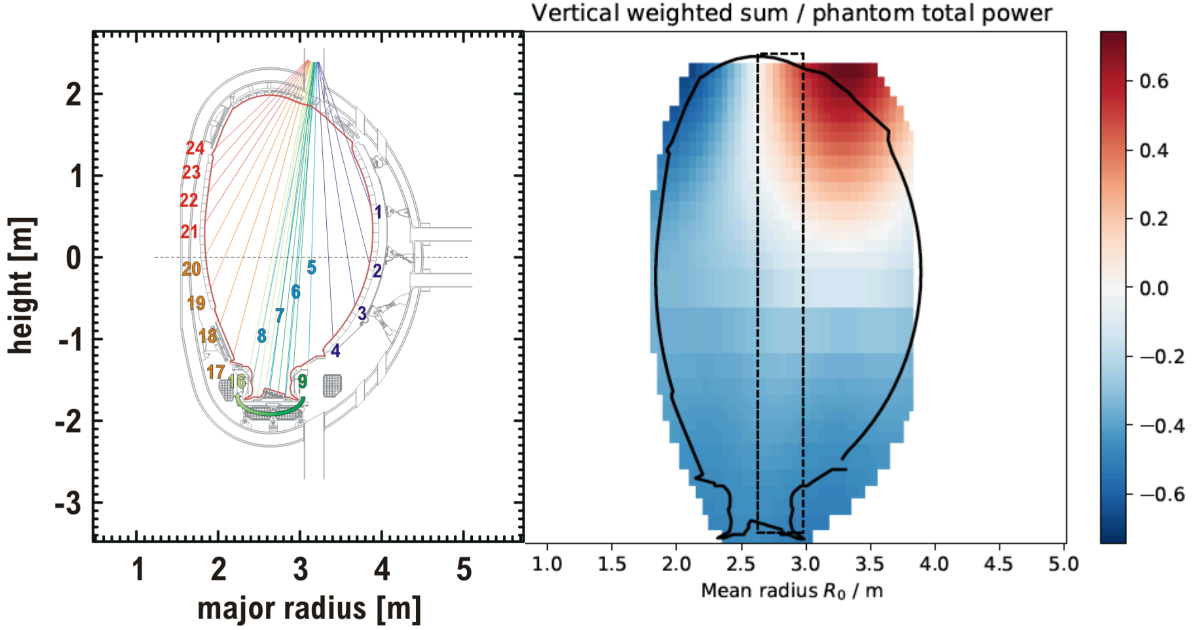

J. Lovell et al., RSI 2020, manuscript in review

Toroidally peaked radiation is expected, so an axisymmetric calculation is unlikely to correctly recover P_{rad} or W_{rad}

- Two bolometer arrays (KB5H and KB5V) operated during JET SPI experiments
- For 3D studies, two measurements toroidally is limiting

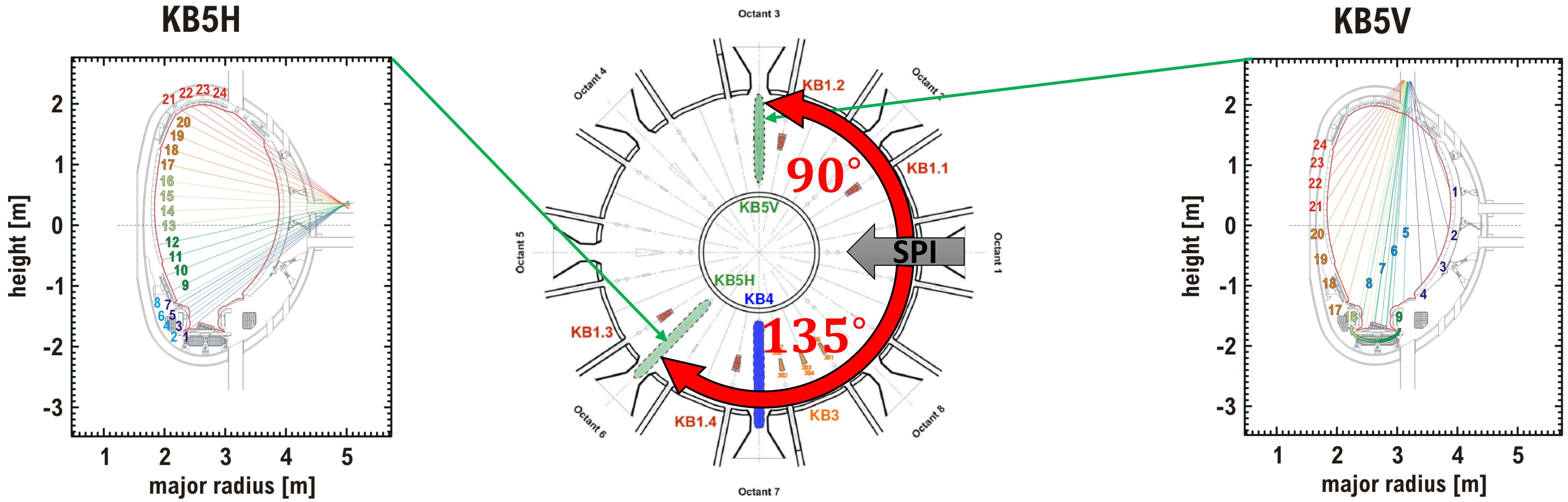

EUROfusion

Helical radiation structures in DIII-D following SPI

Dual SPI experiments revealed the first empirical evidence that the dominant TQ radiation is helical

- Upper and lower AXUV arrays able to locate the peak radiation in one poloidal plane

- Peak radiation regions approximately map to the injection locations

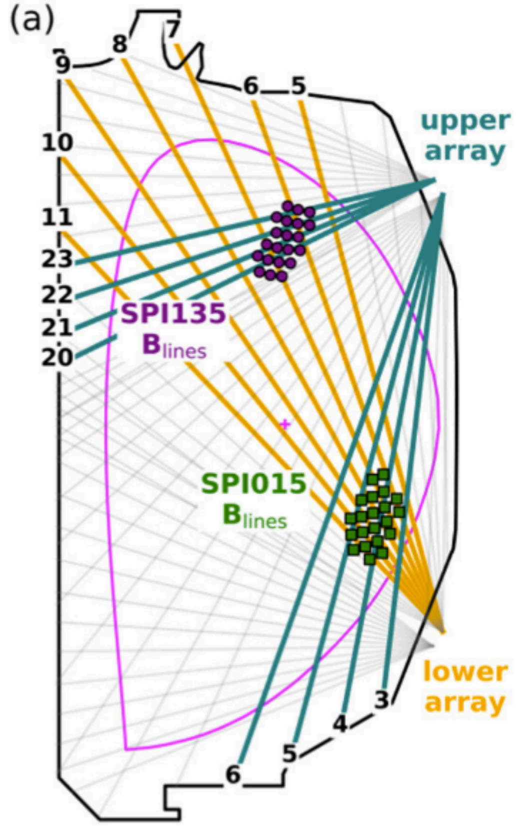

J. Herfindal et al., NF **59** (2019) 106034

Reproducibility of two toroidally separated AXUV brightness contours suggests an ordered structure

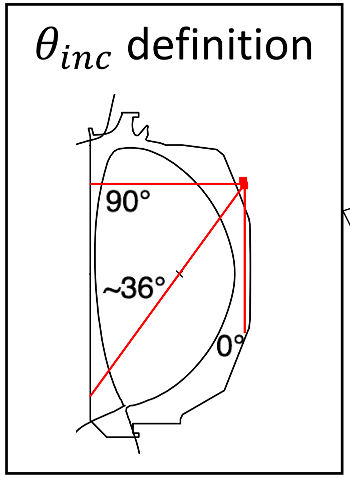

- Typical AXUV brightness contours following 53 Pa m³ Ne SPI into Super H-mode

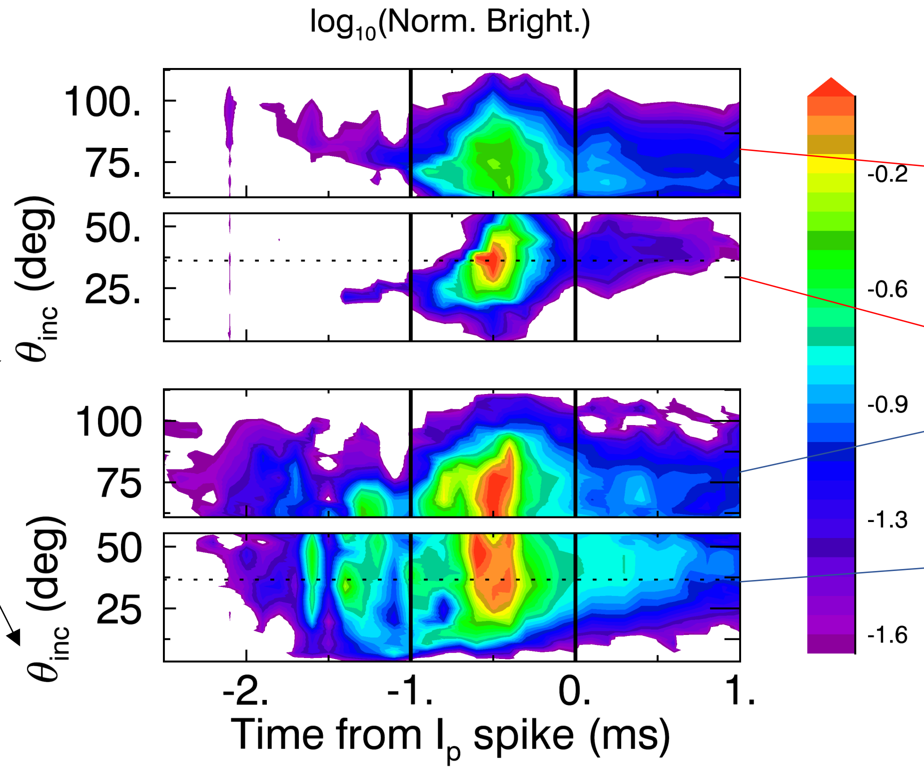

- Geometry of the diagnostics, and example field lines for mapping

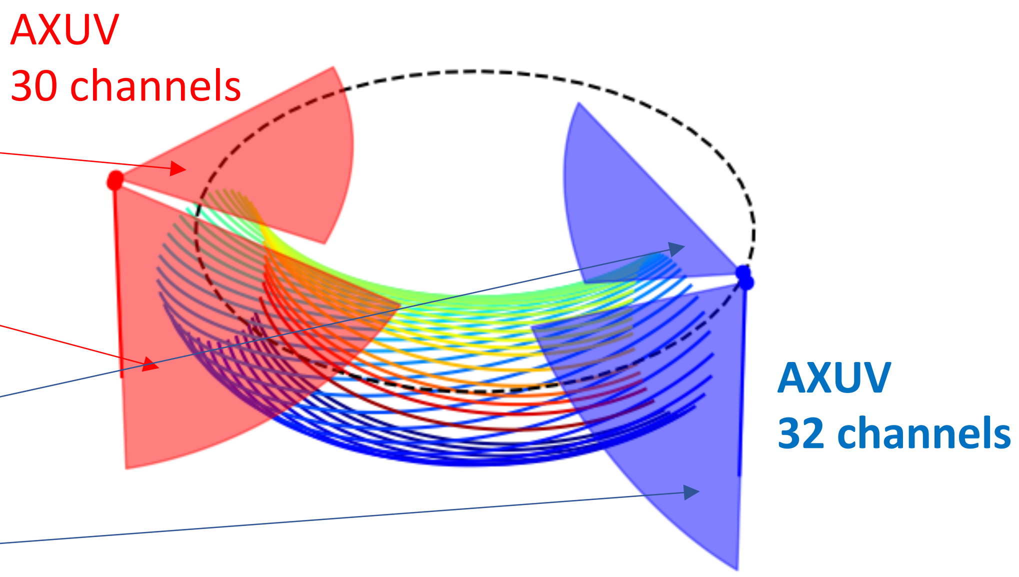

Post-SPI TQ radiation consistent with a helical structure positioned near the 2/1 island X-point

θ_{inc} vs. time space

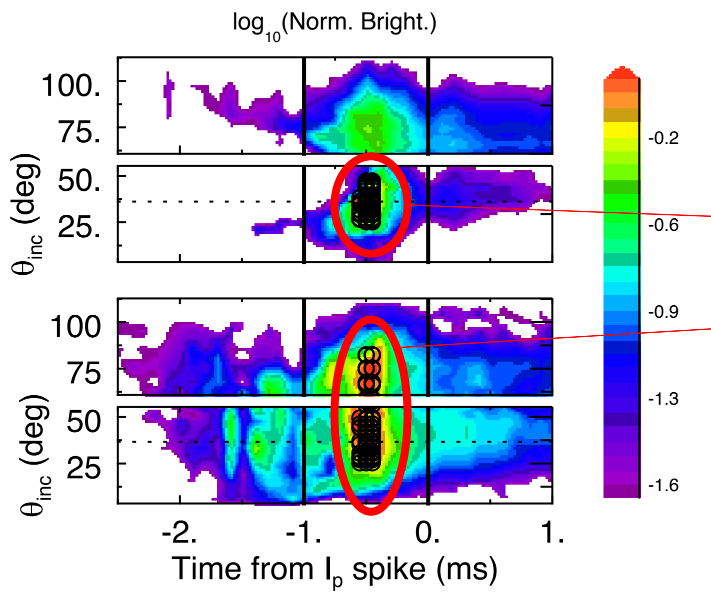

Real space at t=t_{tq}

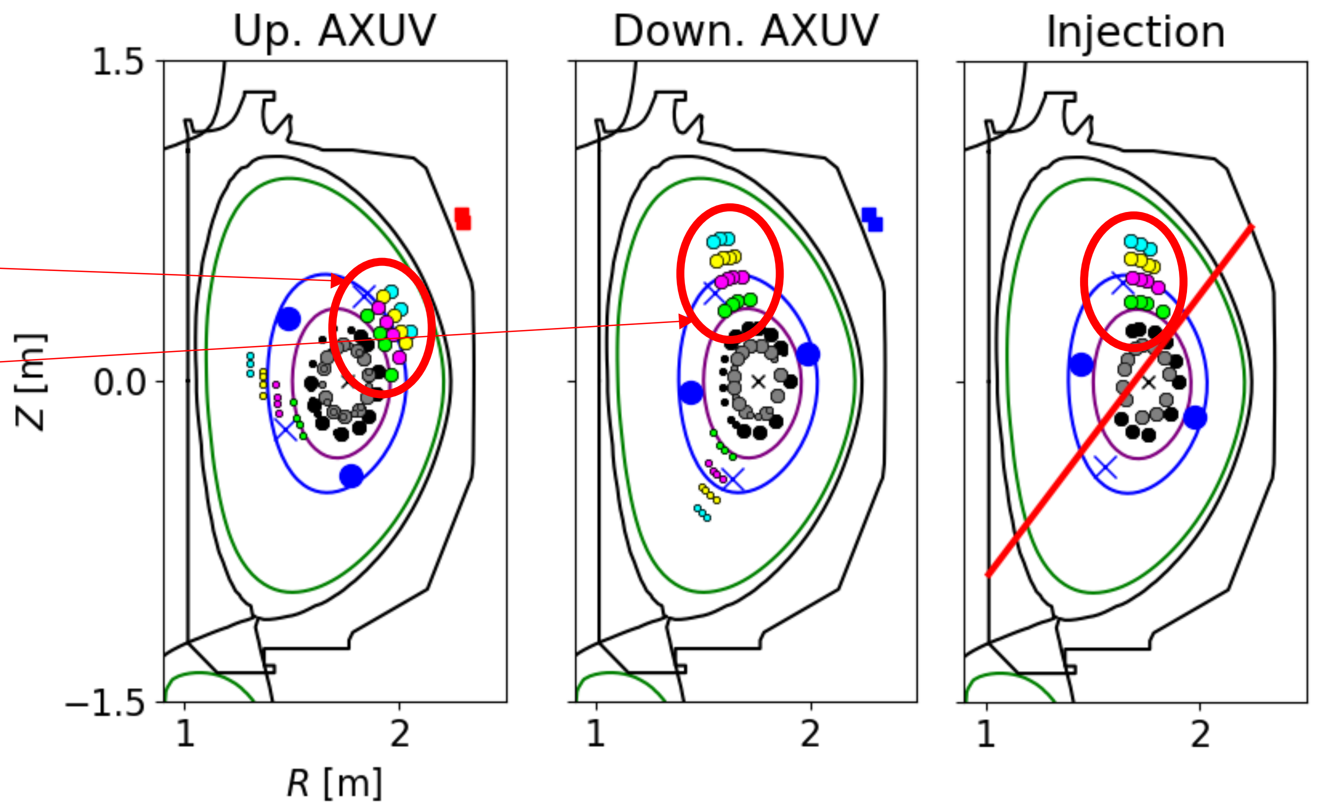

Infrared wall heating is consistent with a toroidally peaked helical structure

- Two identical pellets, two different injectors, two separate discharges
- IR images differenced, field aligned model with Gaussian toroidal dependence fit
- Field pitch matches $\psi_N = 0.4$

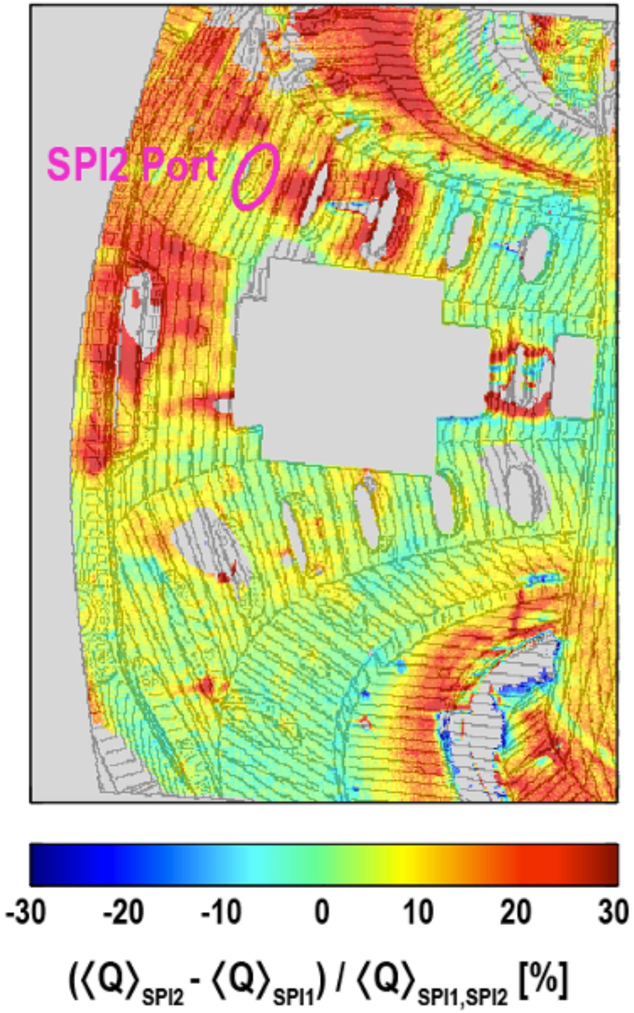

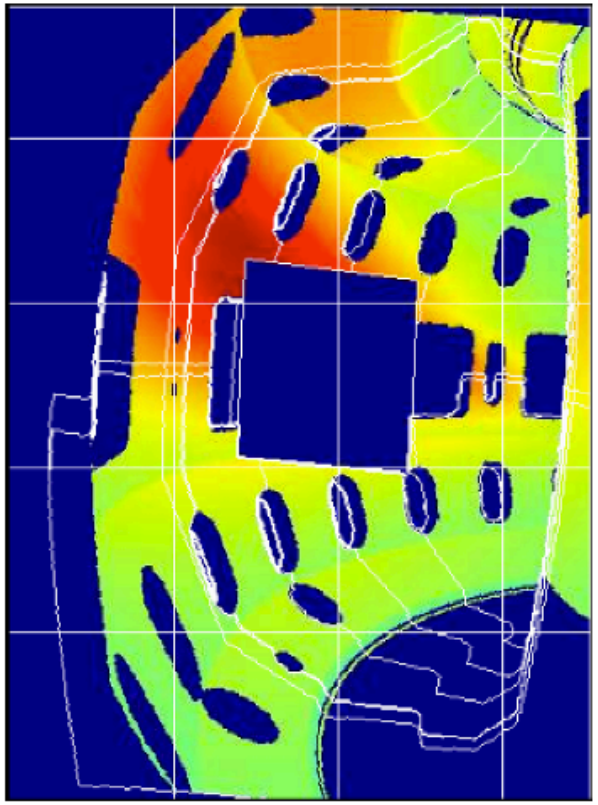

Best-fit, modeled
(PsiN = 0.4, HWHM = 45°)

The calculated toroidal peaking can exceed the ITER limit within the error bar

- **TQ TPF = 1.9 +0.5/-0.3**

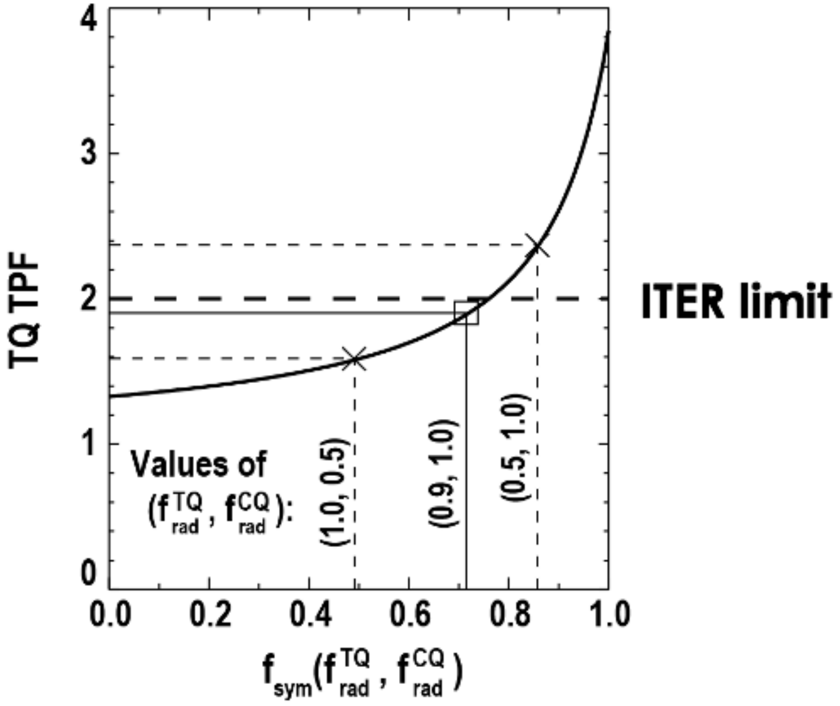

- Poloidal peaking will further increase the total peaking factor PF
- Need methods to reduce the asymmetry; multiple injections?

Derived from D. Shiraki, Disruption Task Force Meeting, June 25, 2020

Helical radiation structures in JET following SPI

A toroidal array of vertically viewing bolometers indicates when plasma radiation is not uniform

- Four bolometers distributed toroidally, referred to collectively as KB1
- Partial view in the poloidal plane
- Cannot differentiate between helical structures and toroidal asymmetries

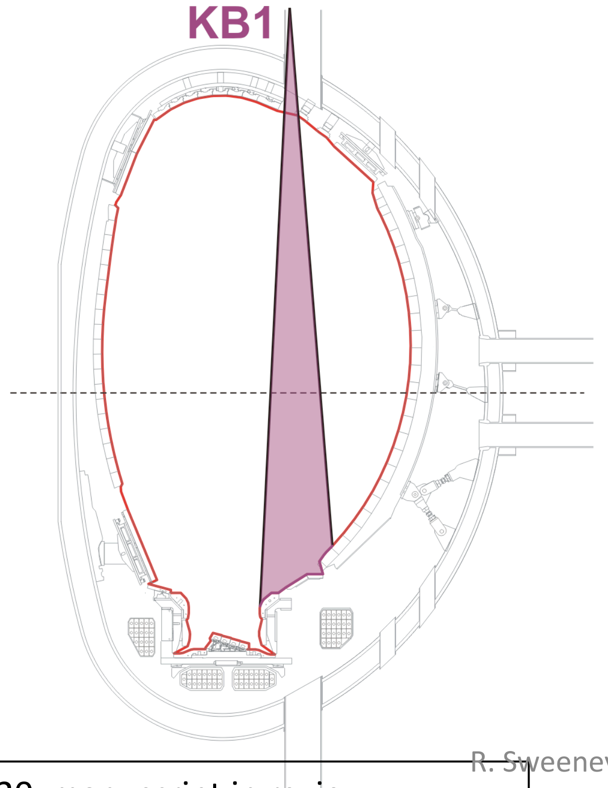

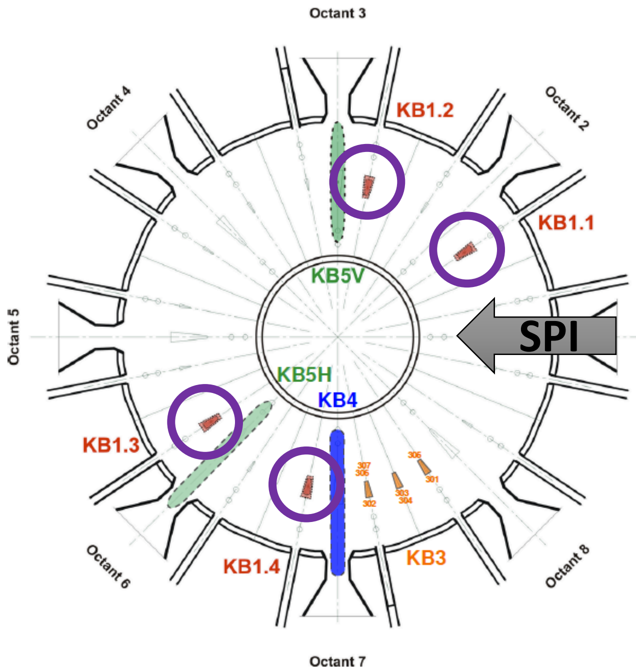

(left) J. Lovell et al., RSI 2020, manuscript in review

When the non-uniformity is large, it is always observed in octant 2 nearest the SPI

- Define a parameter f_{peak} to quantify peaking:

$$f_{peak} = \frac{\max(\Delta Q_i)}{\mathrm{mean}(\Delta Q_i)}$$

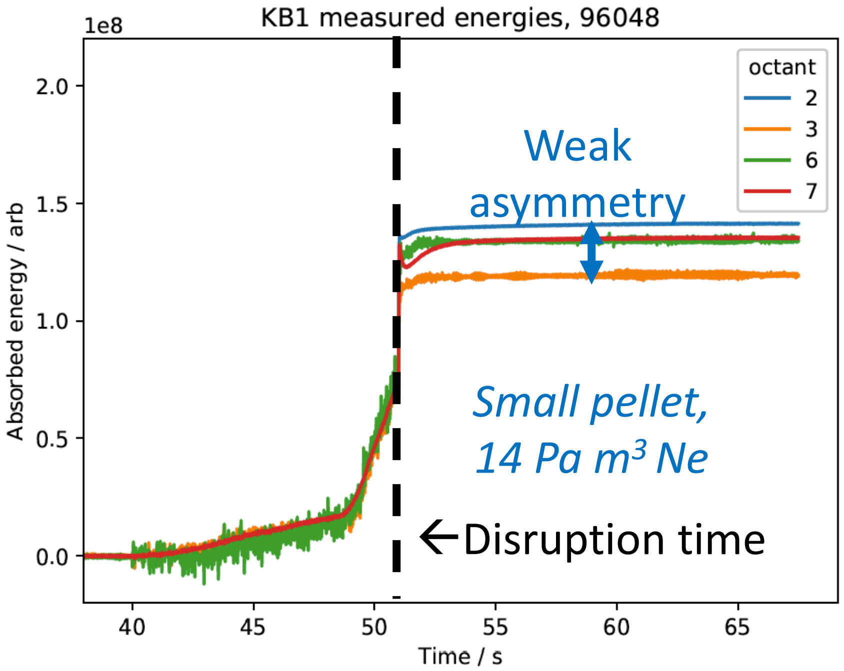

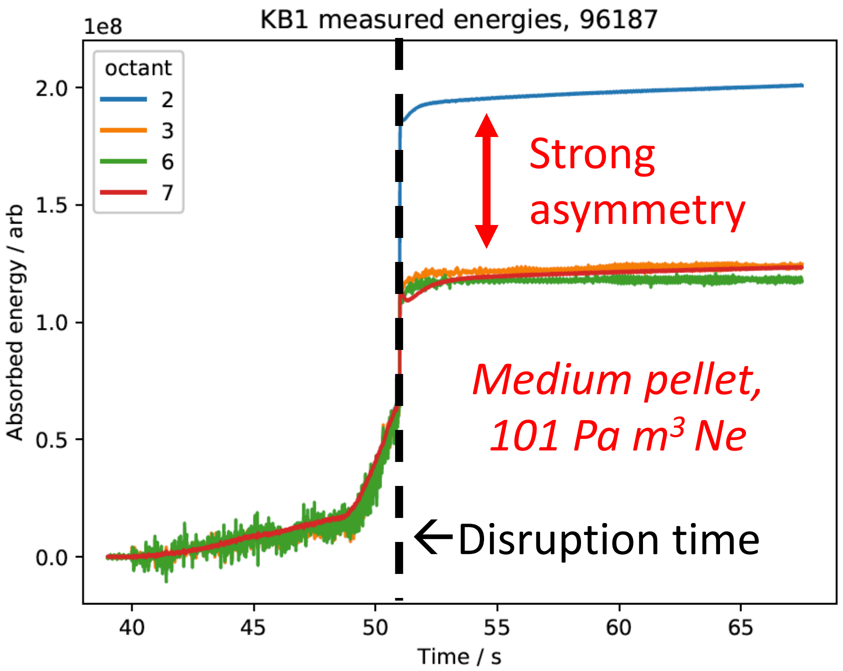

J. Lovell et al., RSI 2020, manuscript in review

The measured **asymmetry** is correlated with the **axisymmetric** <f_{rad}> at fixed neon quantity

- Suggests a systematic error in the axisymmetric <f_{rad}> calculation
  - Can this explain the decreasing <f_{rad}> with f_{th}?

$$< f_{rad} > = < W_{rad} > / (W_{th} + W_{mag} - W_{coupled})$$

$< X >$ ≡ X is calculated assuming axisymmetry

Pure Ne medium pellet

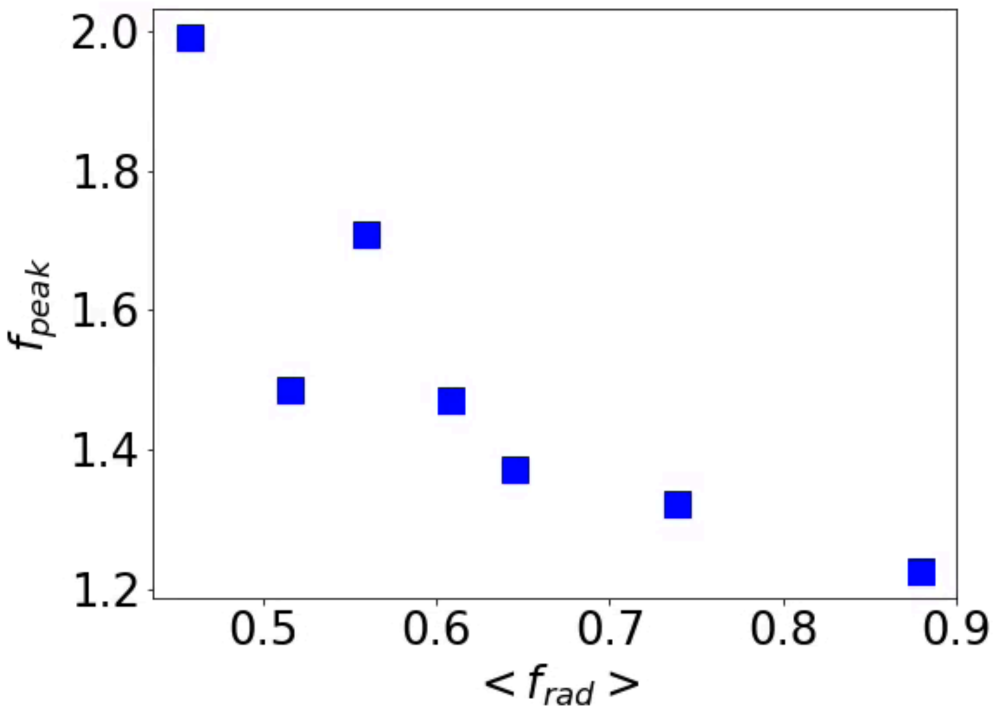

(left) J. Lovell et al., RSI 2020, manuscript in review

If we assume the radiation is helical, the KB1 bolometers place a strong constraint on the emissive structure

KB1 Constraints:

- Helix must intersect KB1 Oct 2
- Helix must not intersect KB1 Oct 3,6, and 7
- Upper region satisfies requirement

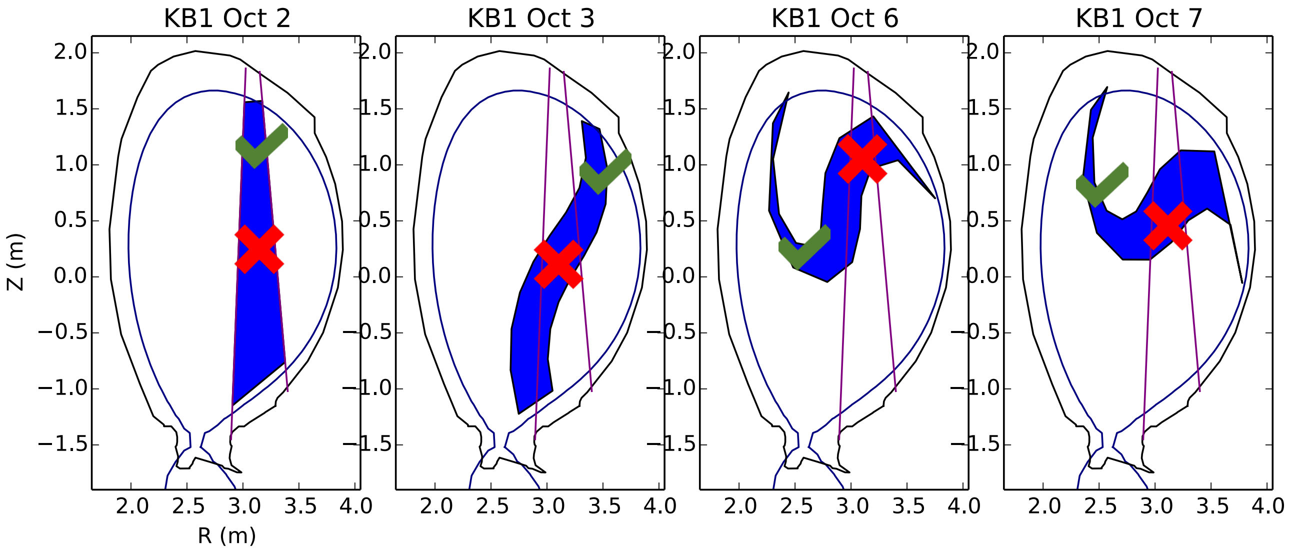

If we assume the radiation is helical, the KB1 bolometers place a strong constraint on the emissive structure

KB1 Constraints:

- Helix must intersect KB1 Oct 2
- Helix must not intersect KB1 Oct 3,6, and 7 ✖
- Upper region satisfies requirement ✔

Emission at injection and KB5s:

- Emission must **overlap** blue and **avoid** red, green, and cyan

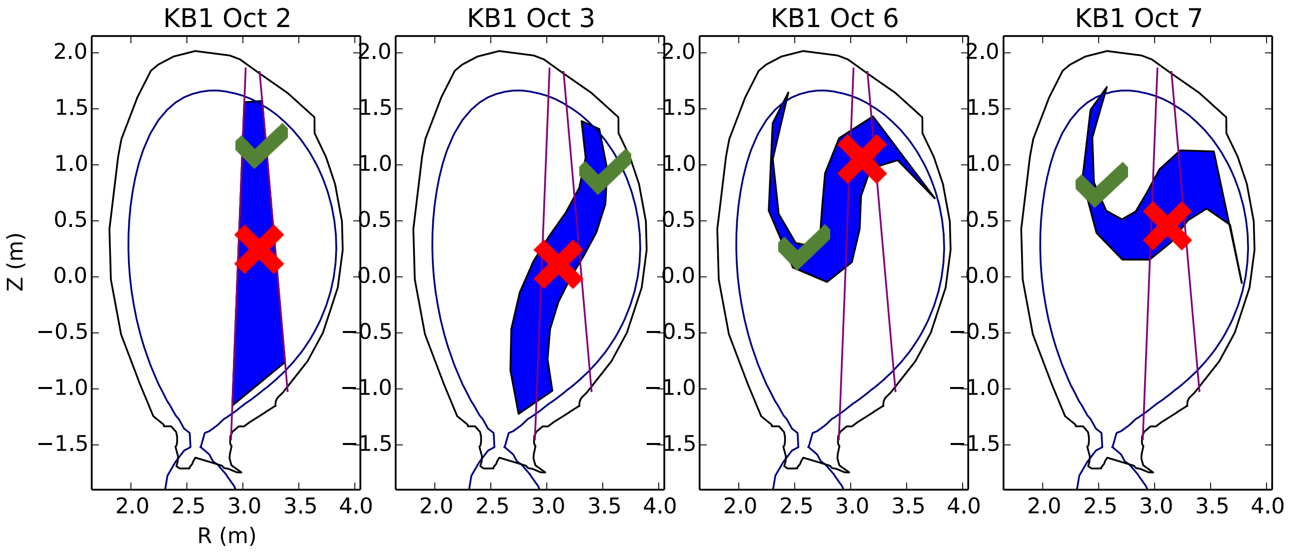

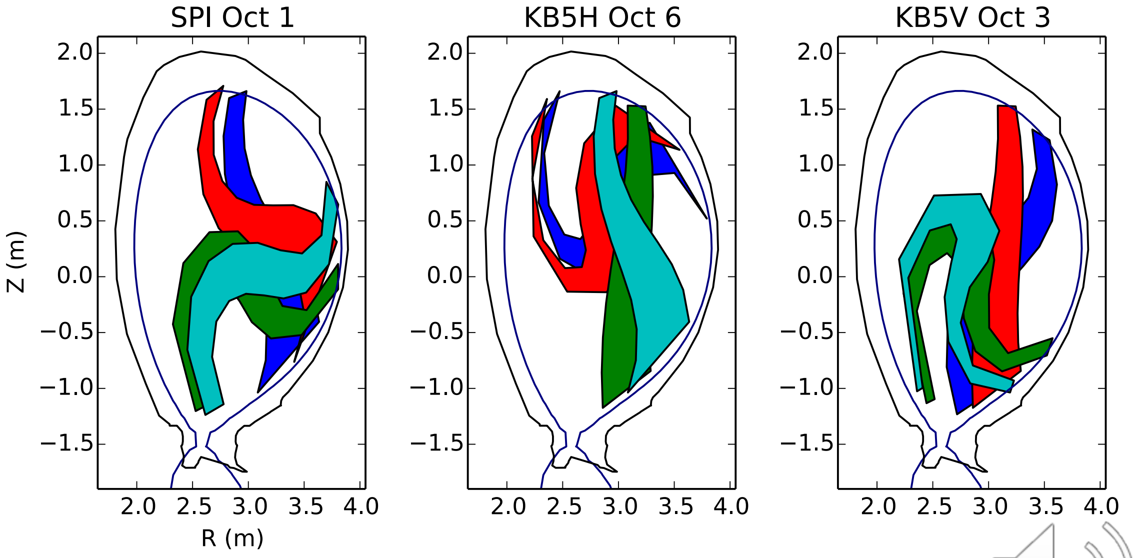

If we assume the radiation is helical, the KB1 bolometers place a strong constraint on the emissive structure

KB1 Constraints:

- Helix must intersect KB1 Oct 2
- Helix must not intersect KB1 Oct 3,6, and 7 ✗
- Upper region satisfies requirement ✓

Emission at injection and KB5s:

- Emission must **overlap** blue and **avoid** red, green, and cyan
- Emission constrained

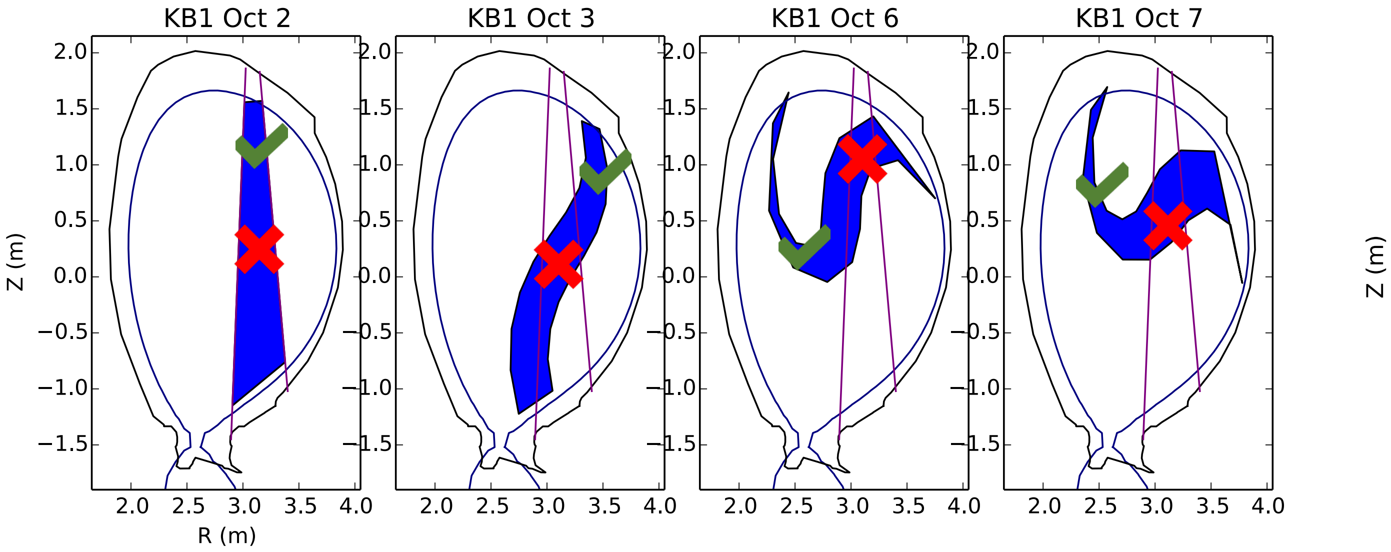

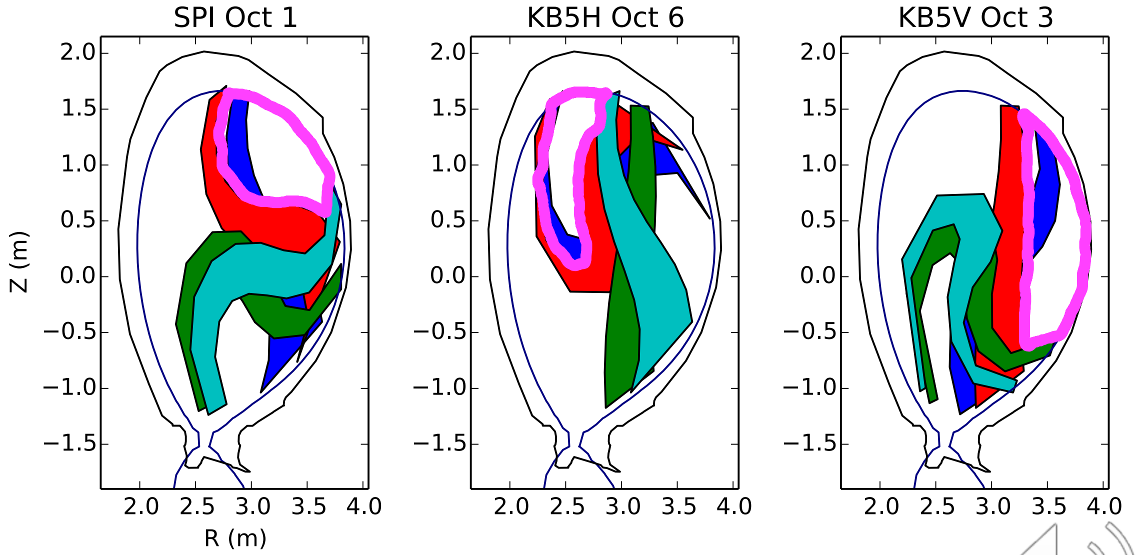

An example helical structure is constructed for 3D radiated power esimates

1. Choose field line satisfying KB1 constraint
2. Bivariate Gaussian assumed in RZ about the field line
3. Fit toroidal Gaussian centered at injection to KB5 measurements

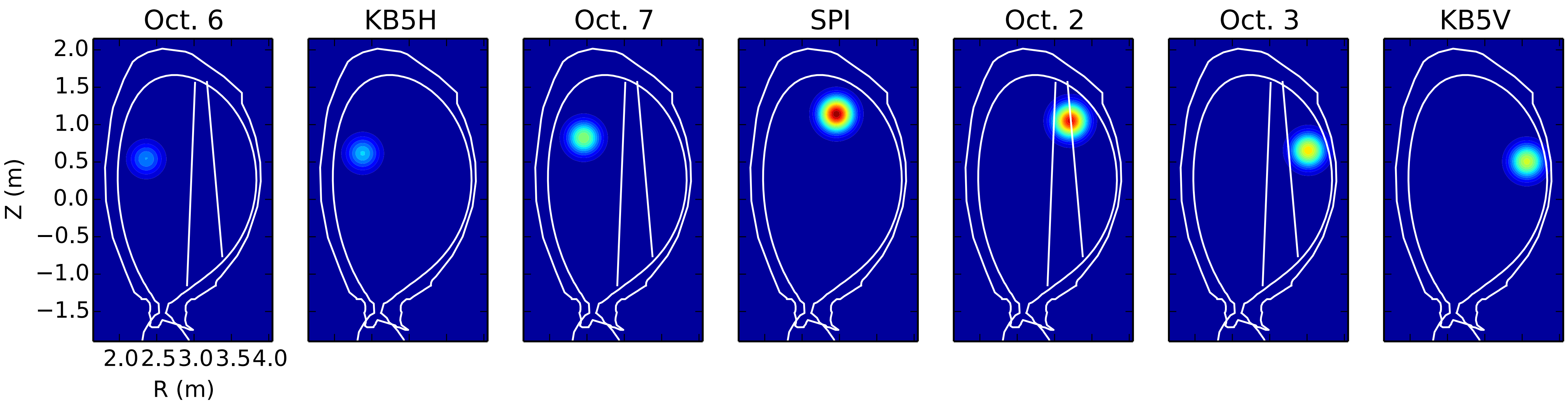

Using the example structure P_{rad} corrections are found

- Small corrections to the standard P_{rad} weighted sums **for this structure**
  - Sensitivity study planned

Correction ≈ −5%

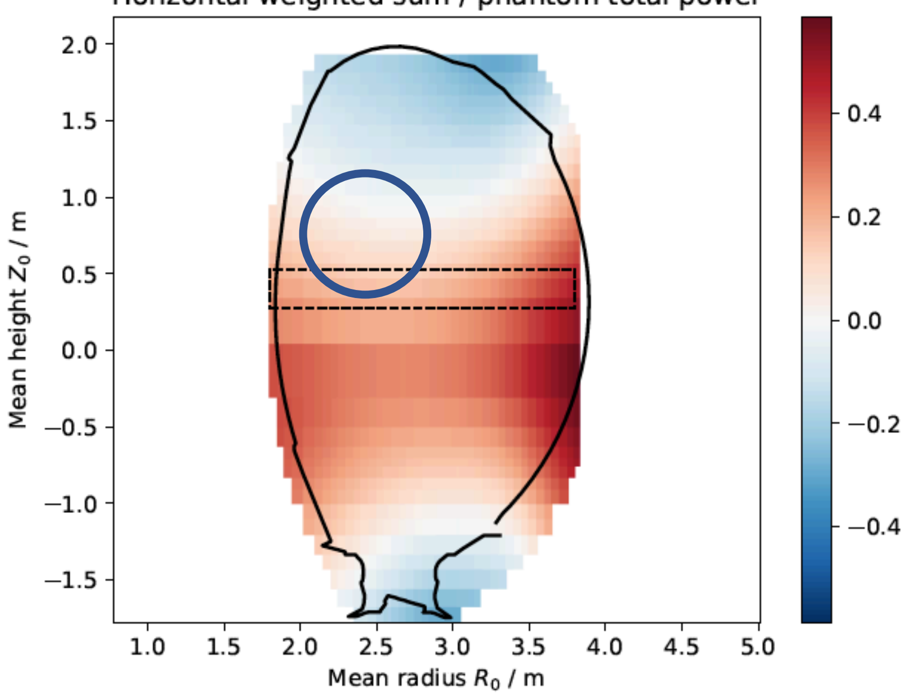

Correction ≈ −5%

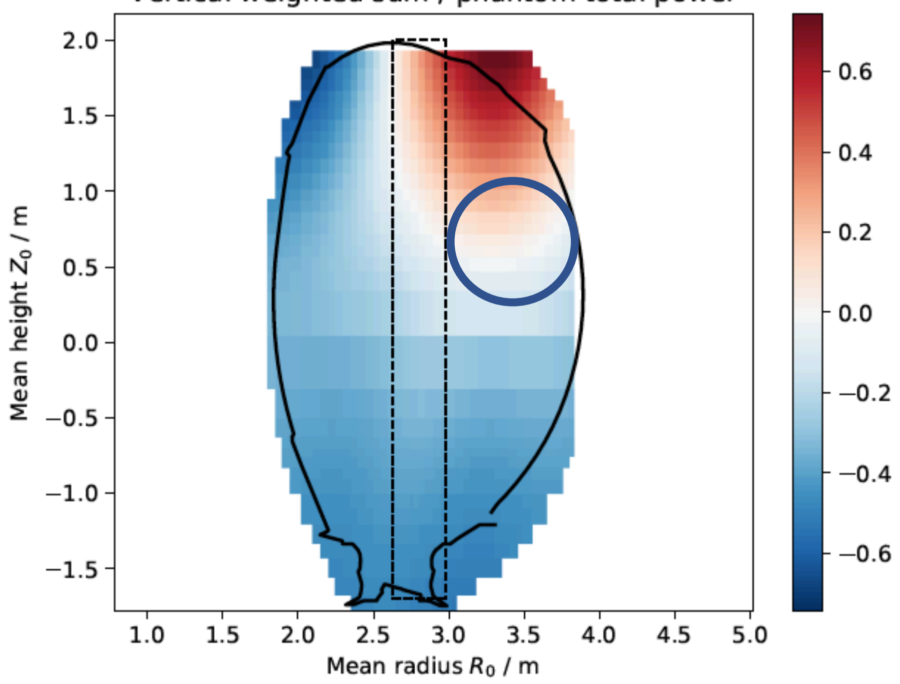

J. Lovell et al., RSI 2020, manuscript in review

Using the corrected KB5s, and assuming axisymmetric CQ radiation, a *preliminary* radiated power from the 3D structure is found

- Toroidal Gaussian fit at times up to current spike
- **Axisymmetric** analysis used **after current spike**

Next steps:

- Vary helical structure within measurement constraints
- Try different toroidal distributions

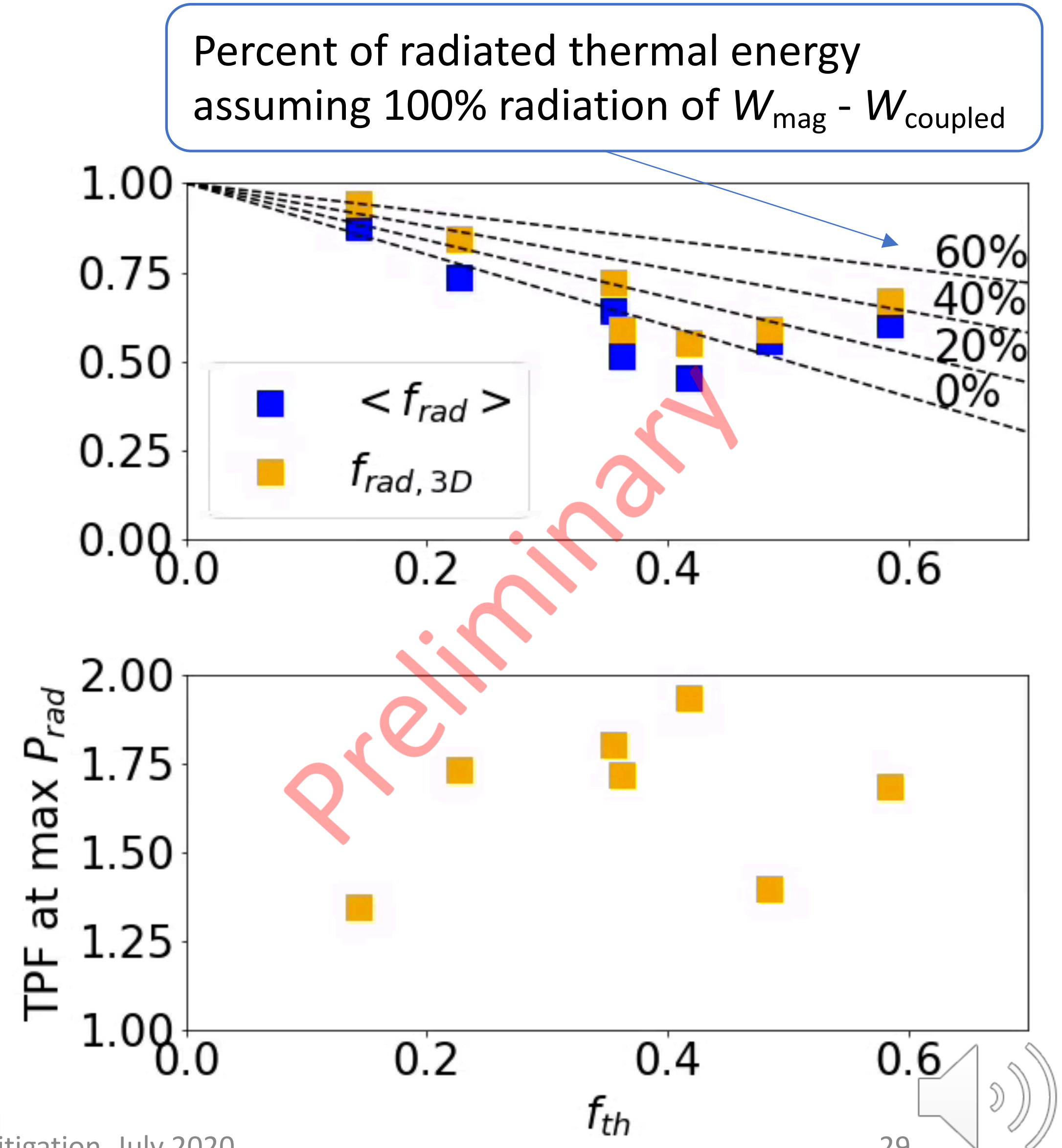

Resolving the toroidal peaking near the injection

KSTAR will be the first device to measure the radiation 11° from the injection; closest measurement to date is 45°

Slide derived from J. Kim

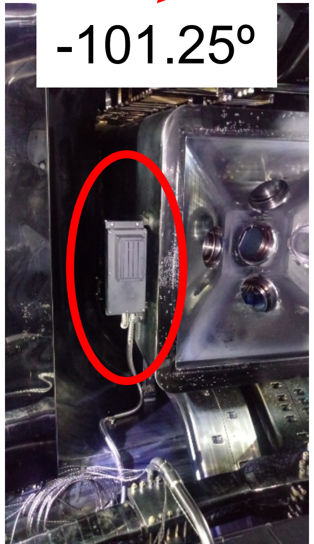

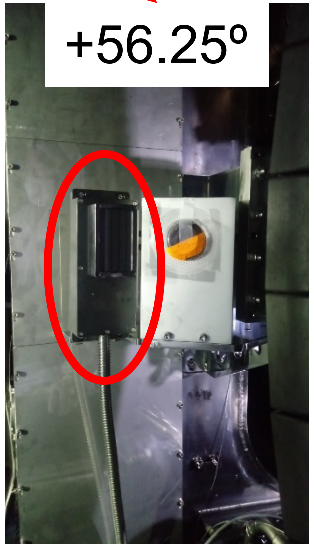

Magnetic control of the radiation asymmetry

Applied EF does not have the same influence in SPI shots

- During MGI, EF can completely determine MHD phase
- During SPI, MHD is strongly influenced by SPI location

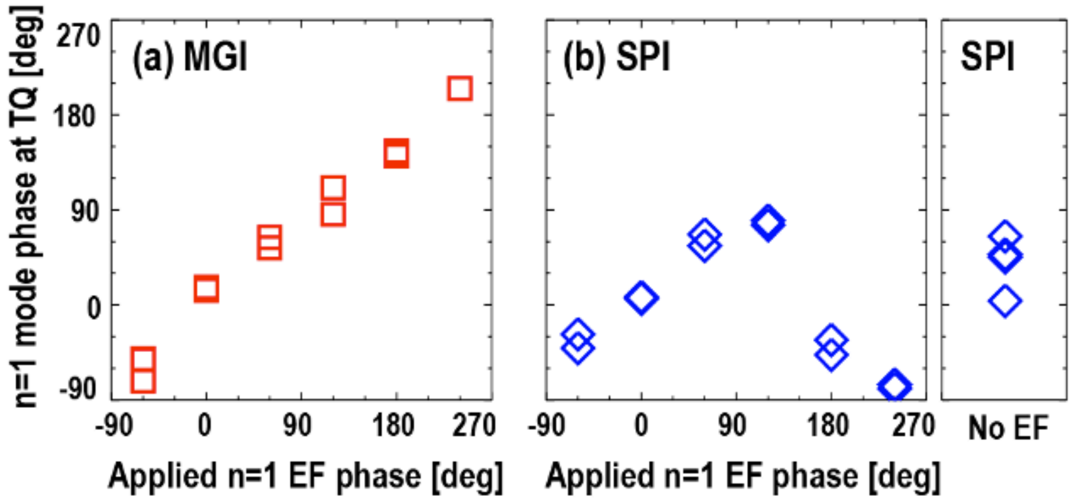

Initial results from magnetic control of the asymmetry in SPI terminated H-mode discharges in JET are inconclusive

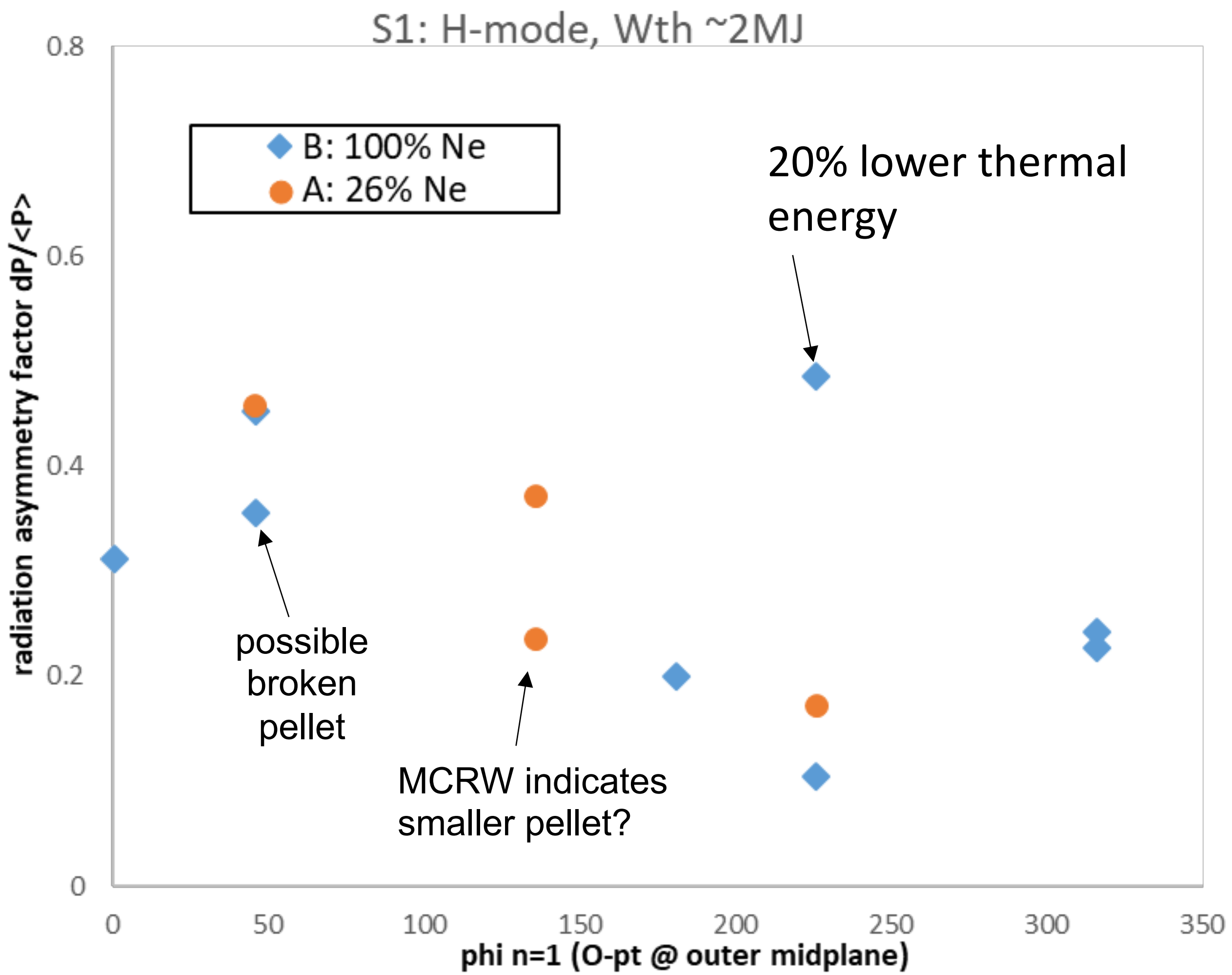

- Minimum at 235 deg?

Or

- No trend?
- This work is ongoing

Slide derived from S. Jachmich M18-34 Report 2020/01/22

In JET Ohmic discharges, the radiation asymmetry appears to reach a minimum at 235 deg following MGI; SPI statistics are low

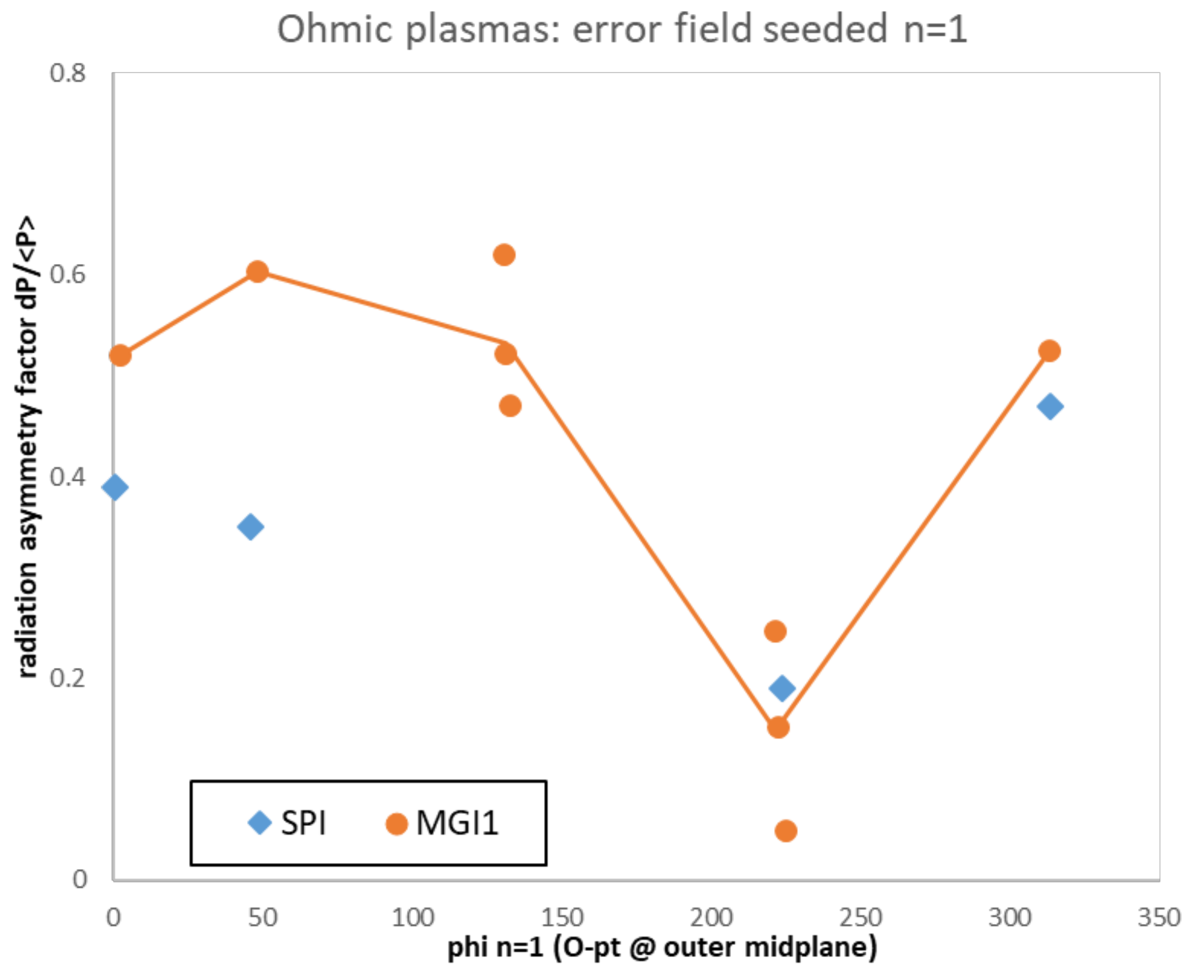

- Is the asymmetry also minimized at 235 deg with SPI?
- Is the electromagnetic perturbation from the injection stronger than the applied EF?

Slide derived from S. Jachmich M18-34 Report 2020/01/22

Radiation following dual injection

DIII-D dual pellet experiment found that simultaneous pellets reduce radiation relative to a single pure Ne pellet

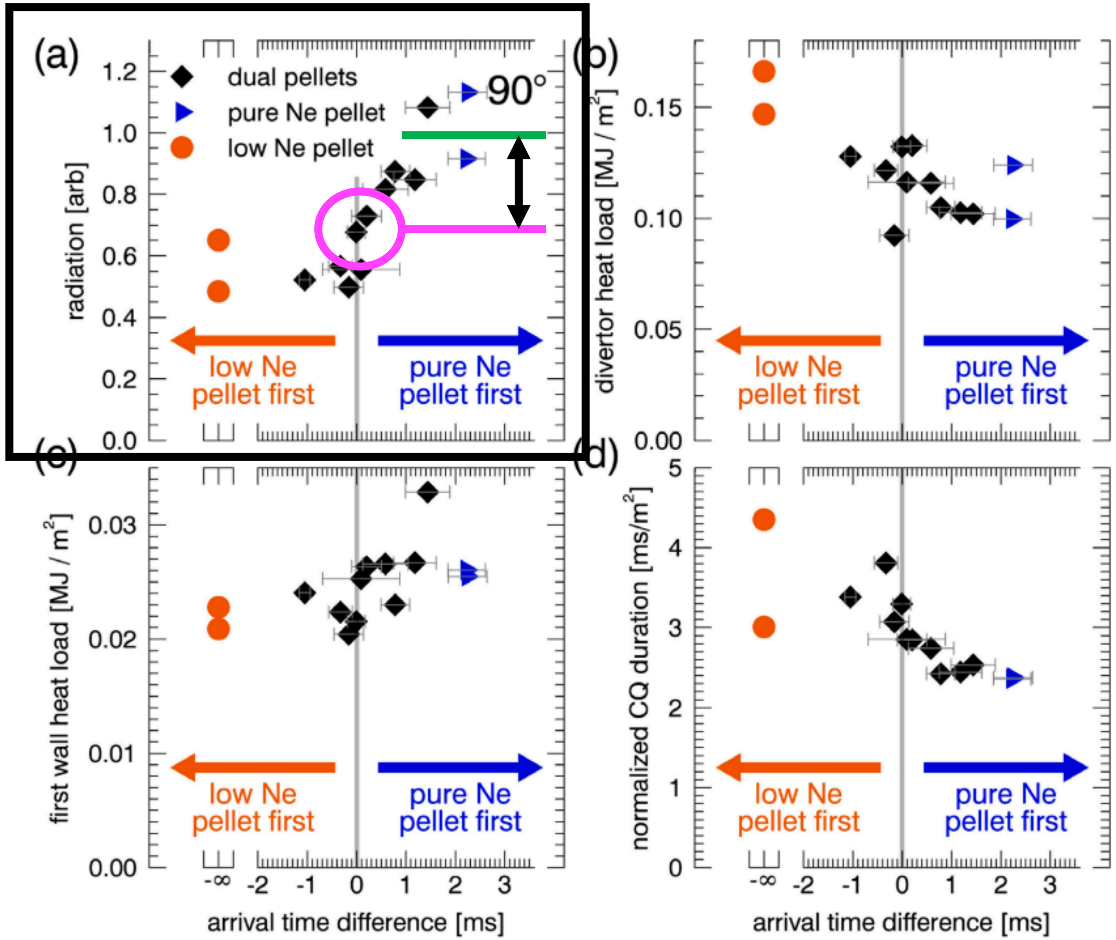

Both 7.5 mm pellets

Low Ne = 1.3 Pa m^3, rest D2

Pure Ne = 53 Pa m^3

At least two possible interpretations:

- *3D effect:* Cooling multiple flux tubes, reducing cooling duration and assimilation
- *0D effect:* Saturating the plasma such that only a fraction of the total material is assimilated

Conclusion

- ITER requires $f_{rad,th}$>0.93 and PF<2
- In DIII-D, axisymmetric thermal fraction $\langle f_{rad,th} \rangle$ approaches 0.9
- Decreasing $\langle f_{rad} \rangle$ observed with increasing f_{th} in JET
- Helical radiation is observed in DIII-D:
  1. Varying injection location changes radiation
  2. Toroidally separated AXUVs consistent with field-aligned structures
  3. IR analysis consistent with helical structure, and predicts TPF=1.9+0.5/-0.3
- Helical radiation is also observed in JET:
  - KB1 bolometers are consistent with a helical structure
- Constrained helical structure used in preliminary 3D radiated energy calculations; predicts $TPF \sim 1.75$ and $f_{rad,th} \sim 0.5$
  - Sensitivity study to follow
- Magnetic control of radiation asymmetry in DIII-D unsuccessful, and JET experiments are inconclusive (more data to come)
- DIII-D dual injection results suggest a reduced f_{rad}; reason under investigation

Extra slides

J-TEXT has a similar diagnostic set to DIII-D and provides a small major radius data point for scalings

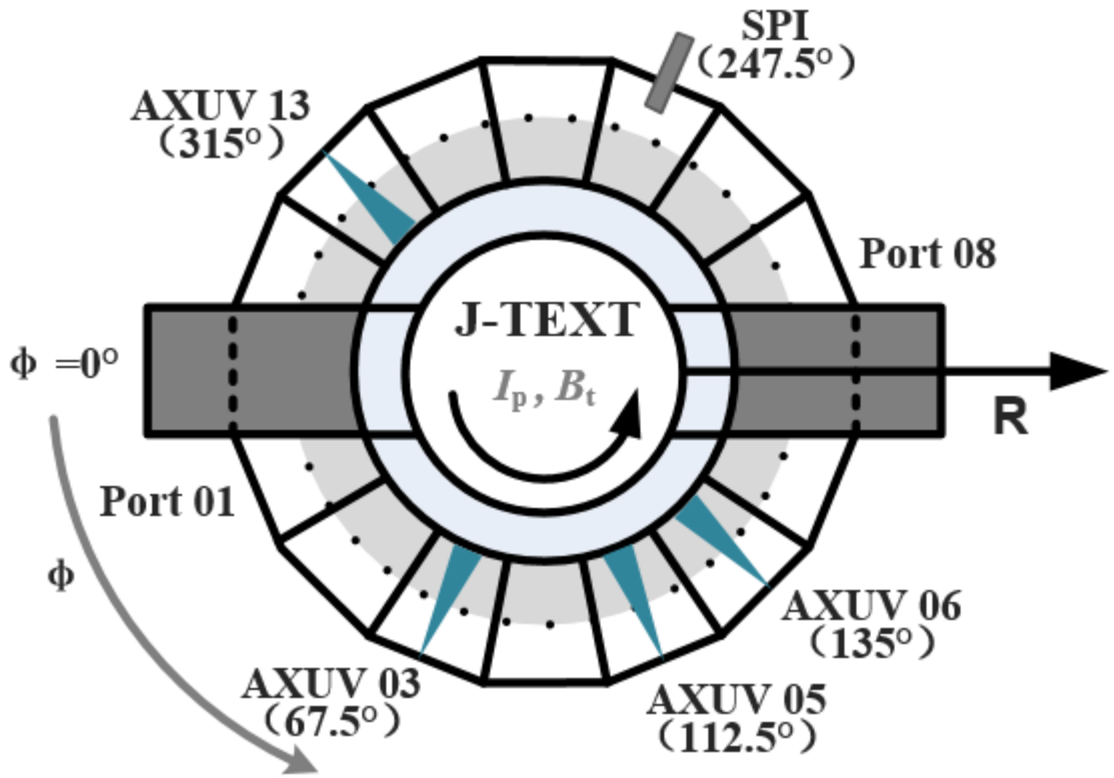

The toroidal position of SPI and AXUV array on the J-TEXT.

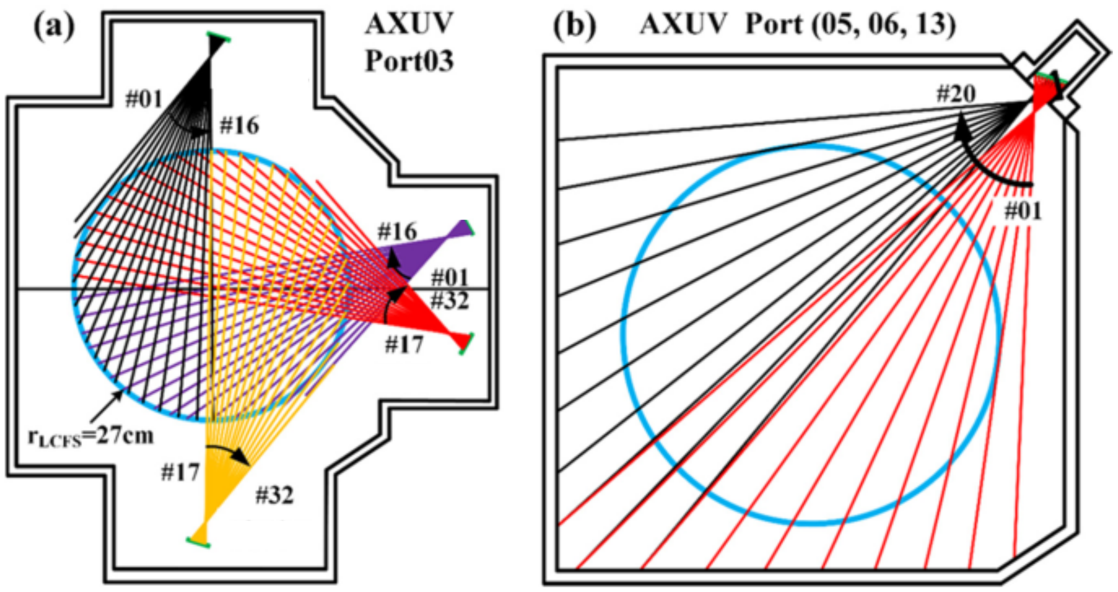

The poloidal layout of the AXUV array on the J-TEXT.

Adapted from slide by You Li

Can the n=1 mode be controlled, and to what degree does the asymmetry depend on its phase?

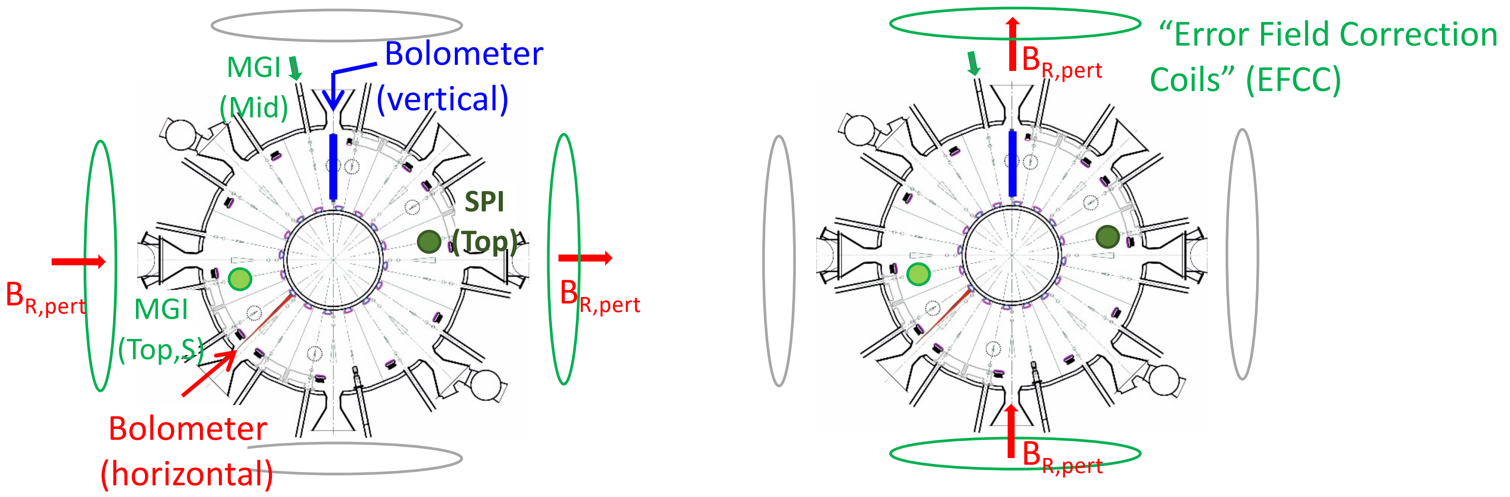

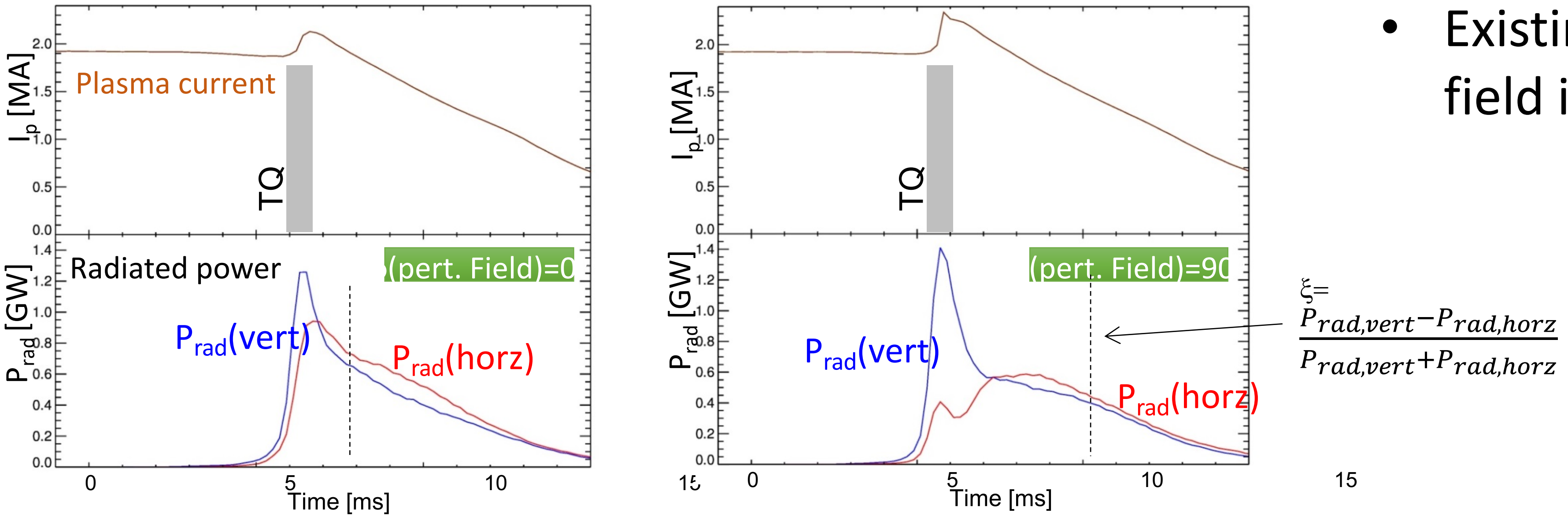

- Coils are sufficient to rotate n=1 fields
- Mode driven by field in L-mode
- Existing mode aligned with field in H-mode

Slide derived from S. Jachmich M18-34 Report 2020/01/22

The SPI births island O-points, determining the initial phase, and perhaps a preferential phase

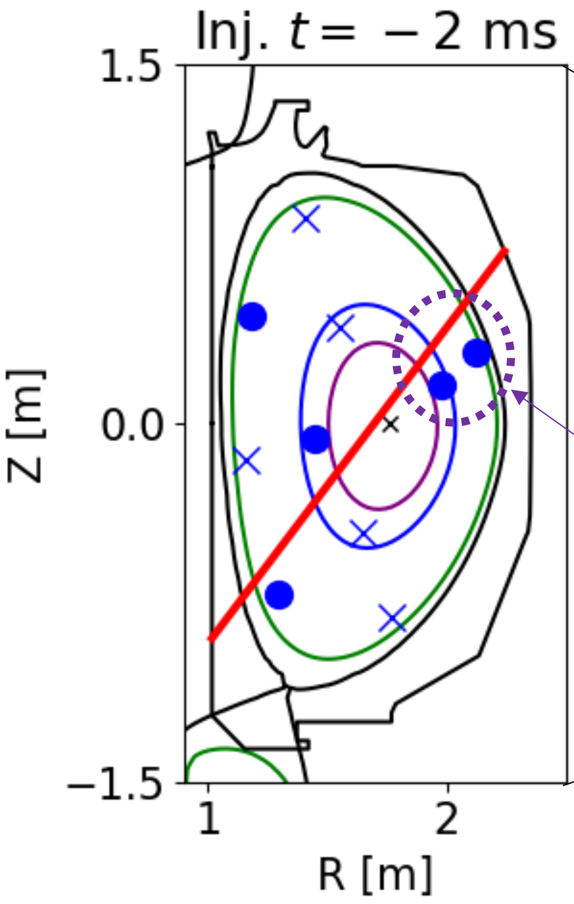

2/1 and 3/1 O-points near injection trajectory

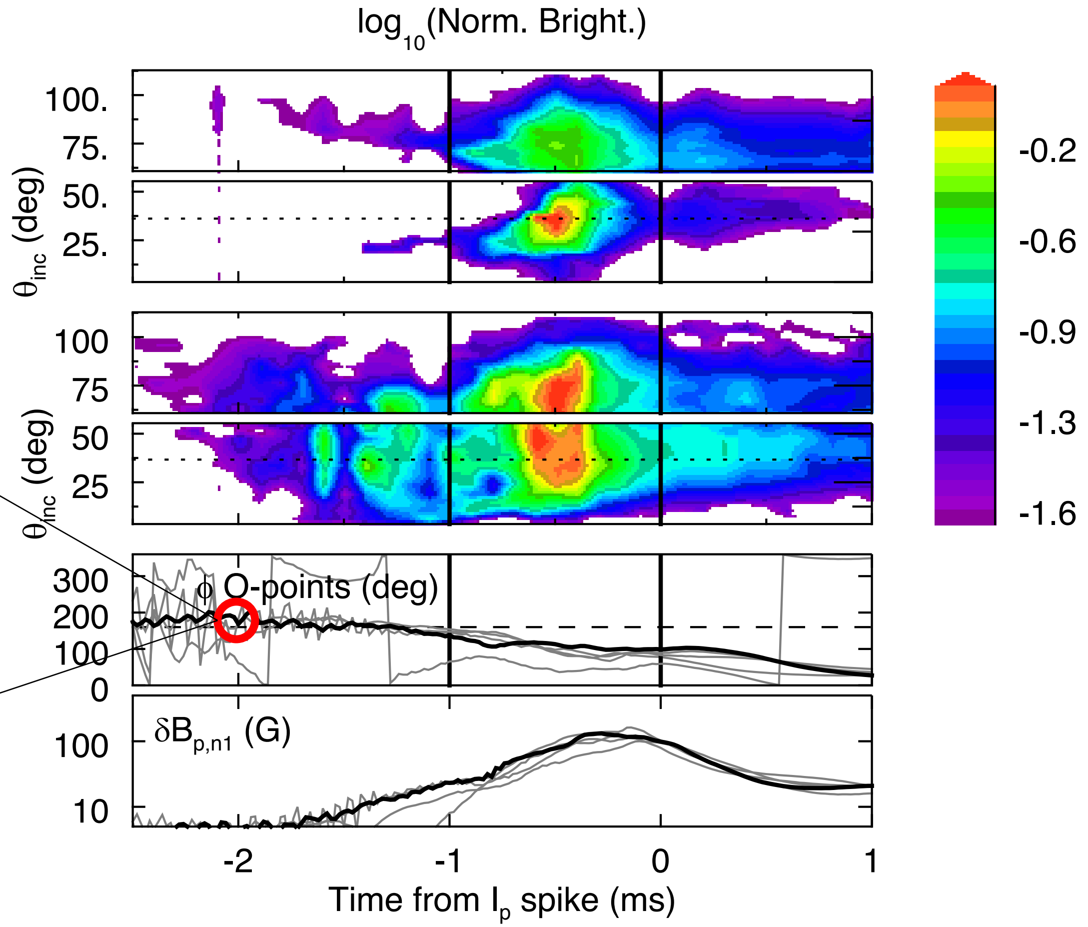

Installation/upgrade of diagnostics are concurrently progressing for investigating the disruption mitigation.

Toroidal AXUV arrays from O-port SPI
#1: +56.25 °
#2: -11.25°
#3: -33.75°
#4: -101.25°

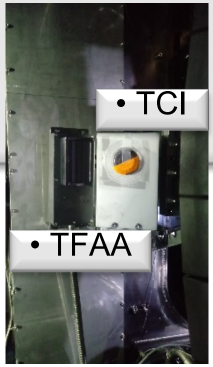

- Filtered AXUV (poloidal and toroidal)
- IR sensor bolometer

SPI

- Divertor IR TV (vertical, 0.25 Mpx@1 kfps)

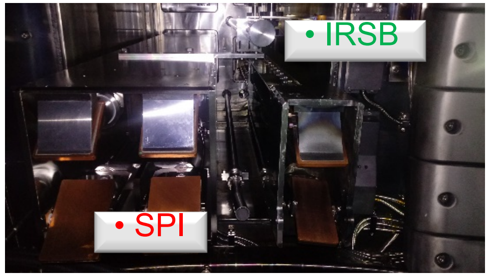

MGI

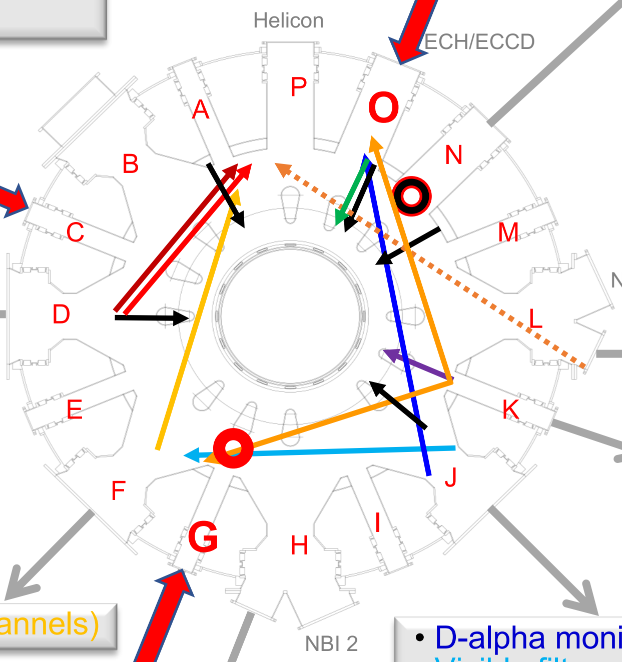

- Filtered AXUV (poloidal)
- Tangential IR TV (100 Hz)
- Imaging bolometer (100 Hz)

- *Fast imaging bolometer (>1 kHz)*

- CCD1 for O-port (10 kfps)
- CCD2 for G-port (10 kfps)
- ECE radiometer

- Two-color interferometer (tangential 5 channels)

- D-alpha monitor (Ne, Ar, He filter)
- Visible filter scope (Ne, Ar, He filter)
- Visible spectrometer

SPI

- ECEI 1 (500 kHz)

- Dispersion interferometer (vertical 3 channels)
- ECEI 2 (500 kHz)

- Hard X-ray monitor
- Neutron detector

Installation status of poloidal AXUV arrays (PFAAs): The PFAAs at D-port and O-port have different design due to the interface.

- The PFAAs at O-port have in-vacuum housing design.
- The signal line is connected through vacuum feedthrough.
- They have their own internal shutter.

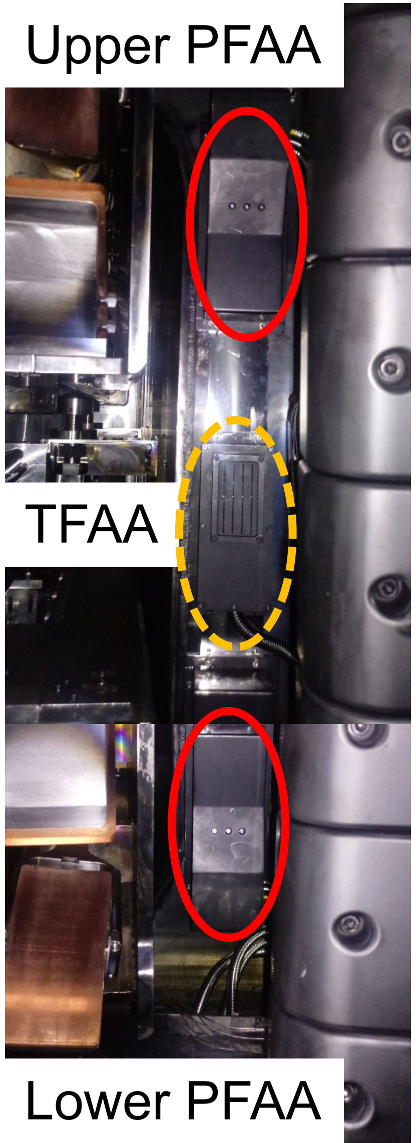

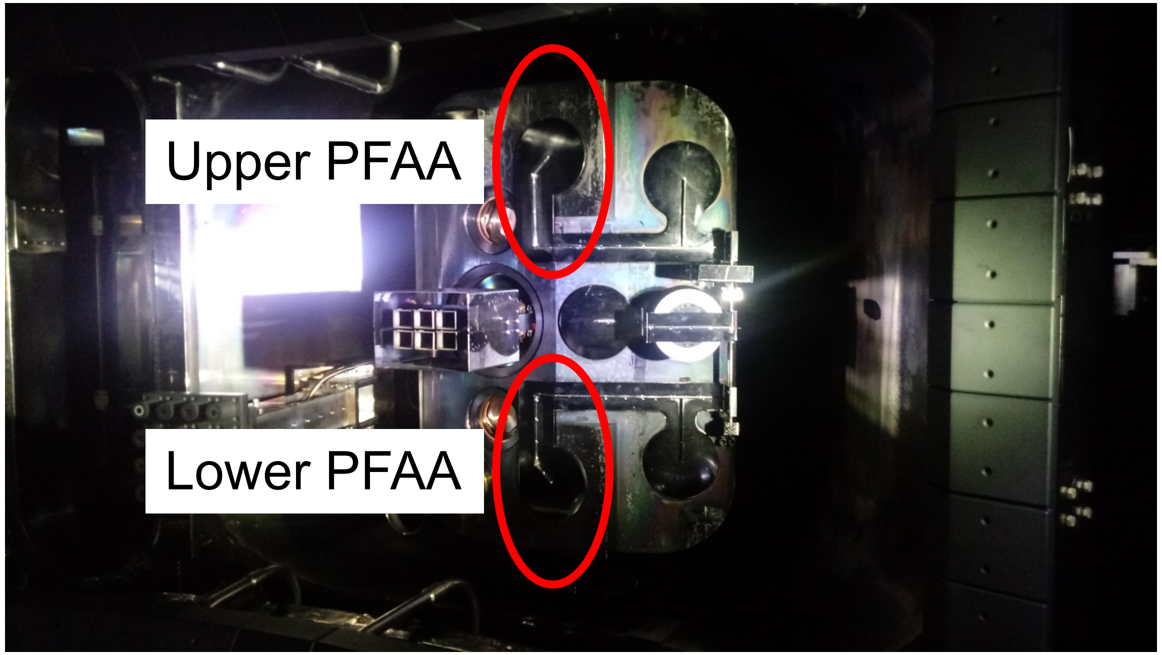

- The PFAAs at D-port have one body design with flange.
- They are protected by external shutter.
- In the figure, the shutter covers the front of PFAAs.

Final design and manufacture of IR sensor based bolometer (IRSB)

Courtesy of G.S. Yun et al.,

* Surface roughness ~ 4 μm

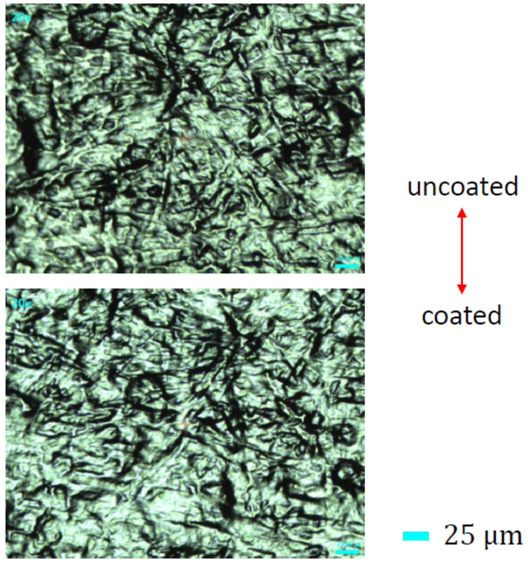

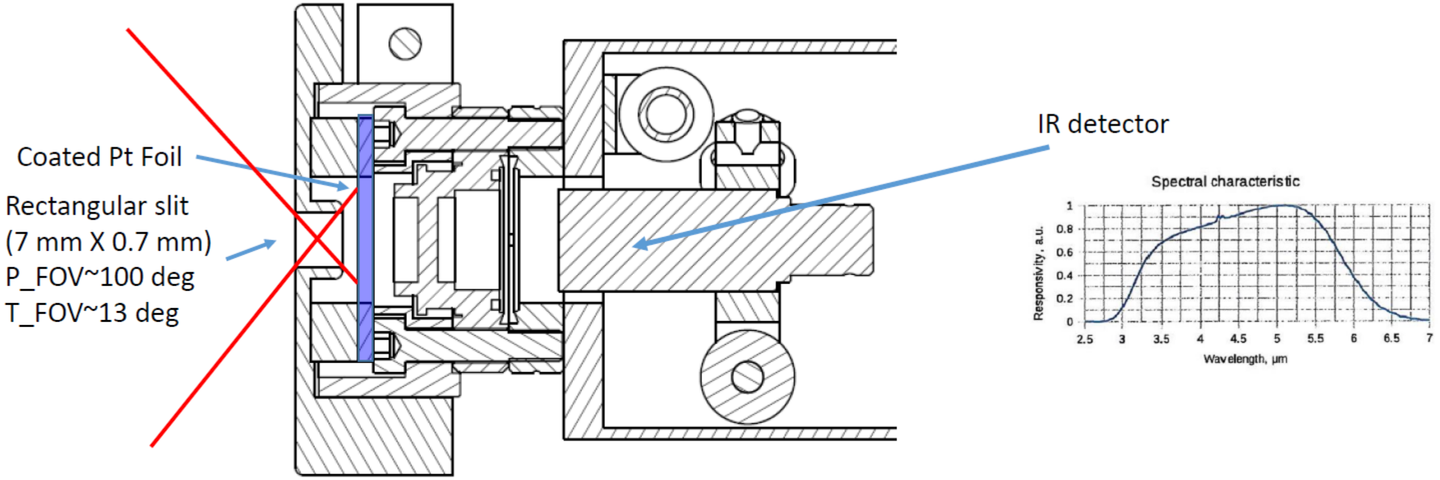

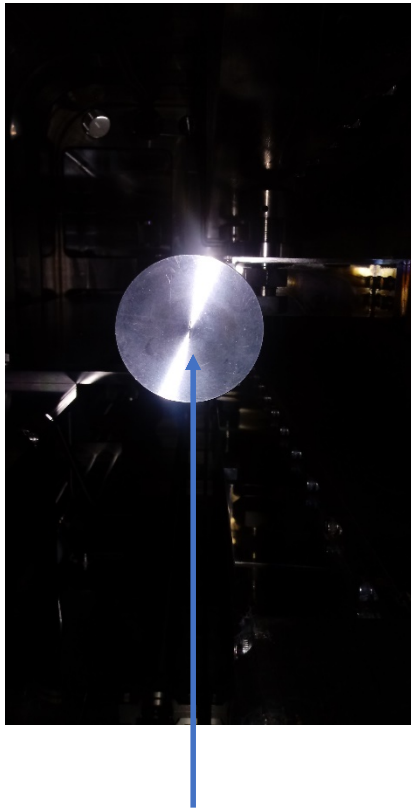

$$\begin{aligned} \text{foil thickness} &= 2.5\mu\text{m} \\ \text{foil diameter} &= 16 \text{ mm} \\ \text{heat capacity} &\sim 1.5 \text{ mJ/K} \\ \text{thermal conductivity} &= 71.6 \times 10^{-3} \text{ W/mm/K} \end{aligned}$$